



# BRNO UNIVERSITY OF TECHNOLOGY

VYSOKÉ UČENÍ TECHNICKÉ V BRNĚ

## FACULTY OF MECHANICAL ENGINEERING

FAKULTA STROJNÍHO INŽENÝRSTVÍ

## ENERGY INSTITUTE

ENERGETICKÝ ÚSTAV

# POSSIBILITIES OF USING MAGNETICALLY ACTIVE LIQUIDS IN MICROFLUIDICS

MOŽNOSTI VYUŽITÍ MAGNETICKY AKTIVNÍCH KAPALIN V MIKROFLUIDICE

## MASTER'S THESIS

DIPLOMOVÁ PRÁCE

## AUTHOR

AUTOR PRÁCE

Bc. Anna Glozigová

## SUPERVISOR

VEDOUCÍ PRÁCE

doc. Ing. Simona Fialová, Ph.D.

BRNO 2024



# Assignment Master's Thesis

Institut: Energy Institute  
Student: **Bc. Anna Glozigová**  
Degree program: Power and Thermo-fluid Engineering  
Branch: Fluid Engineering  
Supervisor: **doc. Ing. Simona Fialová, Ph.D.**  
Academic year: 2023/24

As provided for by the Act No. 111/98 Coll. on higher education institutions and the BUT Study and Examination Regulations, the director of the Institute hereby assigns the following topic of Master's Thesis:

## Possibilities of using magnetically active liquids in microfluidics

### Brief Description:

The thesis will deal with the study of the properties of magnetically active liquids. Nowadays, the popular reduction of the size of test circuits leads to the idea of using microfluidics for testing. The study will also look at the possible use of magnetic fluids to control the stiffness of the fluid layer and the permeability of seals. Design and execution of experiments, corresponding pilot computer modelling and application design.

### Master's Thesis goals:

Based on the research of a comprehensive topic, the student will select the area of the most effective use of microfluidics to change the properties of, for example, dampers, seals or couplings with magnetically active liquid. The student will design a simple experiment and perform a computer simulation using commercially available software to verify the predicted properties. Apply the knowledge acquired in the optimisation of hydrodynamic devices.

### Recommended bibliography:

Karniadakis, G.; Beskok, A.; Aluru, N.: Microflows and Nanoflows Fundamentals and Simulation, ISBN: 978-0-387-28676-1, 2005.

Machů, T.: Pružné spojky na principu tekutin. Brno: VUT v Brně, FSI, 2014, diplomová práce

Jančík, K. Návrh hydrodynamické ucpávky axiálního čerpadla s prstencovým motorem. VUT v Brně, FSI, 2018, diplomová práce.

Přikryl, M. Hydrodynamické tlumiče na principu magnetické kapaliny. VUT v Brně, FSI, 2017, diplomová práce.

Deadline for submission Master's Thesis is given by the Schedule of the Academic year 2023/24

In Brno,

L. S.

---

doc. Ing. Jiří Pospíšil, Ph.D.  
Director of the Institute

---

doc. Ing. Jiří Hlinka, Ph.D.  
FME dean

## **ABSTRACT**

The thesis addresses the topic of magnetically active liquids and their applications in microfluidics. The first part of the thesis comprises an extensive examination of the thematic units that address the issue in question. This part includes a detailed review of the fundamentals of magnetism, magnetically active liquids, and microfluidics, with particular mention of the so-called millifluidics and micromagnetofluidics. This part also presents, among other things, applications and problems associated with instabilities in the lubrication of hydrodynamic plain bearings. The second area focuses on the practical aspects of the research, including the design and implementation of the experiment and the computational simulations performed using FEMM and ANSYS Fluent software. The third section discusses the potential use of magnetically active fluids in millichannels to control undesirable phenomena associated with lubricating oil instabilities in hydrodynamic bearings.

## **KEYWORDS**

Magnetically active liquids, magnetorheological liquid, Bingham, microfluidics, millifluidics, FEMM, journal bearings, lubrication-induced instability

## **ABSTRAKT**

Diplomová práce se zabývá magneticky aktivními kapalinami a jejich aplikacemi v mikrofluidice. V první části práce je provedena rozsáhlá rešerše tématických celků, které se problematiky dotýkají. Tato část zahrnuje podrobný přehled základů magnetismu, magneticky aktivních kapalin a mikrofluidiky s přihlédnutím k tzv. milifluidice a mikromagnetofluidice. V této části jsou i, mimo jiné, představeny aplikace a problematika nestabilit spojených s mazáním hydrodynamických kluzných ložisek. Druhá oblast je zaměřena na praktickou část, je zde popsán návrh a realizace experimentu, stejně jako výpočtové simulace provedené pomocí softwarů FEMM a ANSYS Fluent. Třetí část obsahuje rozpravu koncept potenciálního využití magneticky aktivní kapaliny v milikanálcích za účelem regulace nežádoucích jevů spojenými s nestabilitami mazacího oleje v hydrodynamických ložiscích.

## **KLÍČOVÁ SLOVA**

Magneticky aktivní kapaliny, magnetoreologická kapalina, Bingham, mikrofluidika, milifluidika, FEMM, kluzná ložiska, nestability mazacího filmu

## ROZŠÍŘENÝ ABSTRAKT

Cílem této práce bylo provést rozsáhlou rešerši daného tématu. Na základě rešerše, navrženého, sestaveného experimentu a počítačových simulací, bylo úkolem vybrat vhodnou oblast efektivního využití mikrofluidiky ke změně vlastností, respektive optimalizaci hydrodynamického zařízení. V dnešním světě je neustálé zmenšování a nanotechnologie neúprosným trendem, který ještě zdaleka nedosáhl svého vrcholu. Jedním z motivačních aspektů je zájem o využití tzv. smart materiálů, mezi které patří i magneticky aktivní kapaliny, v moderních technologiích. Magneticky aktivní kapaliny představují inovativní řešení s širokou škálou využití, a to nejen v oblasti mikrofluidiky. Jejich specifické vlastnosti lze využít k přesnému ovládnutí a manipulaci s kapalinami na mikroskopické úrovni.

Mikrofluidika je rychle se rozvíjející obor, který nabízí revoluční přístupy v biologii, chemii, medicíně a dalších technických oborech. Je již známo, že integrace magnetických tekutin do mikrofluidních systémů vede například k vývoji nových metod manipulace s biologickými vzorky.

Jedním z motivačních faktorů je potenciál těchto kapalin k řešení nebo zlepšení praktických problémů s řízením a stabilizací tekutin v mikrokanálcích. Zejména potenciál magneticky aktivních kapalin kontrolovat nežádoucí jevy a nestability, které se vyskytují v hydrodynamických ložiscích, představuje atraktivní výzvu s reálným využitím v průmyslu. Na rozdíl od jejich dobře zavedených aplikací v biologii, chemii a medicíně je využití magneticky aktivních kapalin v hydrodynamických prvcích stále poměrně neprobádanou oblastí pro průmyslové inovace.

Práce je rozdělena do tří částí, a to na teoretickou část, praktickou část a část diskuze. První část se skládá z rešerše oborů relevantních pro tuto práci. V první kapitole je představen magnetismus. Jsou zde uvedeny veličiny potřebné k popisu magnetického pole, dále je také popsáno chování magnetických materiálů.

Ve druhé kapitole je provedeno komplexní studium magneticky aktivních kapalin, zejména magnetoreologických. Třetí kapitola je věnována atypickým disciplínám mechaniky tekutin, konkrétně mikrofluidice, milifluidice a mikromagnetofluidice. V této kapitole jsou představeny nezbytné koncepty, které je třeba mít na paměti, neboť to, co platí v makrosvětě, nemusí vždy platit v mikroskopickém měřítku apod.

Čtvrtá kapitola seznamuje čtenáře se širokou škálou aplikací a zařízení využívajících magneticky aktivní kapaliny nebo mikrofluidní principy. Je zde také představena vybraná oblast specifického zařízení, která by byla významná pro další kroky, a to hydrodynamická čepová ložiska. Je představena problematika nestabilit spojených s mazáním ložisek.

Pátá a šestá kapitola jsou věnovány praktické části práce. Je zde popsána konstrukce a uspořádání experimentu s řízením tuhosti kapaliny. Hodnoty magnetické indukce a intenzity magnetického pole pro stanovení meze kluzu jsou získány magnetostatickou simulací. V CFD simulaci je magnetoreologická kapalina pod vlivem magnetického pole nahrazena Binghamovým modelem viskoplastické kapaliny, jehož parametry jsou viskozita v neaktivovaném stavu a výše zmíněná mez kluzu. Nahrazení se provádí pomocí UDF. V poslední kapitole je formou diskuse navrženo možné využití magneticky aktivní kapaliny v mikrokanálech pro kontrolu nežádoucích jevů s nestabilitou vyvolanou mazáním v hydrodynamických ložiscích.

Není nutno příliš zdůrazňovat, že dané téma představuje atraktivní výzvu v mnoha ohledech. Navzdory slibnému konceptu, návrhu a sestavení experimentu, faktor, který se zprvu zdál jako zanedbatelný, negativně ovlivnil chod praktické části a tudíž experiment nemohl být dokončen. Nicméně, v práci jsou uvedeny náměty k dalšímu postupu, které povedou k finálnímu měření.

Výpočtové simulace jsou rozděleny na dvě úrovně a to na magnetostatickou v softwaru FEMM, který využívá metody konečných prvků pro úlohy elektromagnetismu a na CFD výpočet v softwaru ANSYS Fluent, který naopak využívá metodu konečných objemů. Jako vstupní parametry pro magnetostatickou simulaci slouží tzv.  $B - H$  křivka použité magnetoreologické kapaliny MRF-132DG od společnosti LORD, geometrie navrženého experimentu a vlastnosti použité cívky. Výstupem z této simulace jsou hodnoty magnetické indukce a intenzity magnetického pole. Hodnoty magnetického pole poslouží jako vstup v druhé úrovni simulace, tj. v CFD. Je využito magnetohydrodynamického modulu, který přesahuje běžné uživatelské schopnosti, a právě zde je zahrnut vliv externího magnetického pole. Hodnoty intenzity magnetického pole jsou využity pro získání hodnot meze kluzu magnetoreologické kapaliny. Ty jsou potom implementovány v UDF binghamského modelu nenewtonské kapaliny. Dále je taktéž pomocí UDF implementována i pohyblivá síť, neboť se očekává translační pohyb ve směru buzení od cívky.

Přínosem této práce je přiblížení poznatků o magneticky aktivních kapalinách, jejich aplikacích v mikrofluidice a podpora interdisciplinárního přístupu kombinujícího inženýrství a různé aspekty fyziky. Získané poznatky slouží jako odrazový můstek pro další fáze výzkumu a poskytnout pevný základ pro možné budoucí aplikace v tomto směru, které mohou vést k významným inovacím v různých technických a vědeckých oblastech.





#### **BIBLIOGRAPHIC CITATION**

GLOZIGOVÁ, Anna. *Possibilities of using magnetically active liquids in microfluidics*. Brno: Brno University of Technology, Faculty of Mechanical Engineering, 2024. Supervisor of master's thesis doc. Ing. Simona Fialová, Ph.D.



I, the undersigned, hereby declare that I wrote this master's thesis by myself under the supervision of doc. Ing. Simona Fialová, Ph.D. All sources have been accurately reported and acknowledged, and they are listed in references. I hereby give consent for my thesis, if accepted, to be available for photocopying and understand that any reference to or from my thesis will receive an acknowledgment.

Anna Glozigová



I would like to express my deepest gratitude to my supervisor doc. Ing. Simona Fialová, Ph.D., for her incredible guidance, insightful comments, considerable encouragement to finish this thesis, and most importantly, for her immense amount of patience.

Anna Glozigová



# Contents

<b>Introduction</b>	<b>18</b>
<b>1 On Magnetism</b>	<b>20</b>
1.1 Magnetic Fields . . . . .	20
1.2 Magnetic Materials . . . . .	24
Diamagnetic Materials . . . . .	24
Paramagnetic Materials . . . . .	24
Ferromagnetic Materials . . . . .	24
Antiferromagnetic Materials . . . . .	24
Ferrimagnetic Materials . . . . .	25
1.3 Magnetic Hysteresis . . . . .	26
<b>2 Magnetically Active Liquids</b>	<b>28</b>
2.1 Composition of Magnetically Active Liquids . . . . .	29
Magnetic Particles . . . . .	29
Carrier Liquid . . . . .	29
Surfactant . . . . .	29
2.2 Magnetorheological and Magnetoviscous Effect . . . . .	30
2.3 Ferromagnetic Liquids . . . . .	31
2.4 Magnetorheological Liquids . . . . .	31
2.4.1 Rheology of Magnetorheological Liquid . . . . .	32
2.4.2 Modes of Operation . . . . .	33
Valve Mode . . . . .	33
Shear Mode . . . . .	34
Squeeze Mode . . . . .	34
Gradient Pinch Mode . . . . .	35
<b>3 Matter of Scale</b>	<b>36</b>
3.1 Microfluidics . . . . .	36
Reynolds Number . . . . .	37
3.2 Millifluidics . . . . .	37
3.3 Micromagnetofluidics . . . . .	37
3.4 Clarification . . . . .	38
<b>4 Applications</b>	<b>39</b>
4.1 Lab-on-a-Chip, Microfluidic Devices and Applicatons . . . . .	39
4.2 Applications of Magnetically Active Liquids . . . . .	40
Biomechanics and Medicine . . . . .	40
Audio Speakers . . . . .	41

Seals . . . . .	41
Brakes . . . . .	42
Fluidic Soft Robots . . . . .	42
Dampers . . . . .	43
Other . . . . .	43
4.3 Lubrication-Induced Instabilities in Journal Bearings . . . . .	44
Oil Whirl . . . . .	45
Oil Whip . . . . .	45
Dry Whip . . . . .	45
Prevention of the Instabilities Occurrence . . . . .	46
<b>5 Simulations</b>	<b>47</b>
5.1 FEMM Simulation . . . . .	48
5.1.1 Boundary Conditions . . . . .	48
5.1.2 Geometry . . . . .	49
5.1.3 Case Setup and Calculation . . . . .	49
5.1.4 Results and Post-process . . . . .	50
5.2 ANSYS Fluent Simulation . . . . .	53
5.2.1 Geometry and Computational Mesh . . . . .	53
5.2.2 Calculation Configuration in ANSYS Fluent . . . . .	53
<b>6 Experimental Setup Necessities</b>	<b>56</b>
6.1 The Inclined-Tube Micromanometer . . . . .	56
6.2 The Coil . . . . .	57
6.3 LORD MRF-132DG . . . . .	63
6.4 The Method . . . . .	65
<b>7 Discussion</b>	<b>70</b>
7.1 The Experiment . . . . .	70
7.2 Usage Proposal - A Concept Idea . . . . .	71
<b>Conclusion</b>	<b>73</b>
<b>List of Figures</b>	<b>81</b>
<b>List of Tables</b>	<b>83</b>



# Introduction

The purpose of this chapter is to introduce the reader to the motivation behind this work and its objectives. A brief methodological approach used in the composition of the thesis and also in the development of the computational simulation is presented here.

## Motivation

Nowaday's, miniaturisation and nanotechnology are a relentless trend that is far from reaching its peak. One aspect of motivation is the interest in using so-called smart materials, which include magnetically active liquids, in modern technology. Magnetically active liquids are innovative solutions with a wide range of applications, not only in the field of microfluidics. Their specific properties can be used to precisely control and manipulate liquids at the microscopic level.

Microfluidics itself is a rapidly developing field offering revolutionary approaches in biology, chemistry, medicine, and other engineering disciplines. It is already known that the integration of magnetic fluids into microfluidic systems leads, for example, to the development of new methods for manipulating biological samples.

Another motivating factor is the potential of these liquids to solve or improve practical problems of fluid control and stabilisation through microchannels. In particular, the ability of magnetically active liquids to control undesirable phenomena and instabilities that occur in hydrodynamic bearings presents an attractive challenge with real applications in industry. In contrast to their well-established applications in biology, chemistry, and medicine, the use of magnetically active liquids in hydrodynamic components is still a relatively unexplored area with considerable potential for innovation and industrial improvement.

## Objectives

One of the objectives of the thesis is to conduct comprehensive research on a multidisciplinary topic. In this research, the topics of magnetism, magnetically active liquids, microfluidics and various applications are introduced.

Another objective of the research is to study hydrodynamic devices and to select a suitable region for optimisation using magnetically active liquids in microchannels.

Finally, the objective is to design and implement a simple experiment, accompanied by a pilot computer simulation using commercially available software, to verify the predicted properties.

## Methods

The thesis is divided into three parts, namely the theoretical part, the practical part, and the discussion part. The first part consists of research into the disciplines relevant to this thesis. The

first chapter introduces magnetism. The quantities necessary to describe the magnetic field are given, the behaviour of magnetic materials is also described.

In the second chapter, a comprehensive study of magnetically active liquids, in particular magnetorheological and ferromagnetic liquids, is carried out. This chapter includes a list of several manufacturers and an extensive list of applications.

The third chapter is devoted to fluid mechanics disciplines at micro- and millirange. The first part introduces the necessary concepts of microfluidics, as what is true in the macro world is not always true at the microscopic scale. Micromagnetofluidics and so-called millifluidics are also mentioned as they are relevant for this work as well.

The fourth chapter introduces the reader to a wide range of applications and devises using magnetically active liquids or microfluidic principles. A selected area of the specific device that would be considerable for the next steps, namely hydrodynamic journal bearings is presented here as well. The issue of instabilities associated with bearing lubrication is introduced.

The fifth and sixth chapters are devoted to the practical part of the thesis. The design and setup of the liquid stiffness control experiment are described. The values of magnetic induction and magnetic field strength to determine the yield stress are obtained by magnetostatic simulation. In the CFD simulation, the magnetorheological liquid under the effect of the magnetic field is replaced by a Bingham model of viscoplastic liquid, whose parameters are the viscosity in the unactivated state and the aforementioned yield stress. The replacement is done by the UDF. The last chapter discusses the experiment procedure. Also, a proposal of possible use of the magnetically active liquid in microchannels to control undesirable phenomena with lubrication-induced instabilities in hydrodynamic bearings is carried out here.

## **Contribution**

The contribution of this work is to bring closer the knowledge of magnetically active liquids and their applications in microfluidics and to promote an interdisciplinary approach combining engineering and various aspects of physics. The knowledge gained can serve as a springboard for further steps of research, providing a solid foundation for possible future applications in this direction that can lead to significant innovations in various engineering and scientific fields.

# Chapter 1

## On Magnetism

This chapter provides a summary of the essential characteristics required to describe the magnetic field. This chapter is primarily based on the following sources: [1], [2], [3], [4], [5], [6].

### 1.1 Magnetic Fields

A magnetic field is an area where magnetic forces are applied. Depending on its nature, the magnetic field can be divided into stationary and non-stationary. A stationary field is a time-variant field, while a non-stationary field is always characterised by variability in time.

Magnetic fields occur, for example, around magnetised substances, and they can be described graphically by magnetic field lines (sometimes referred to as magnetic induction lines), see the following figure:

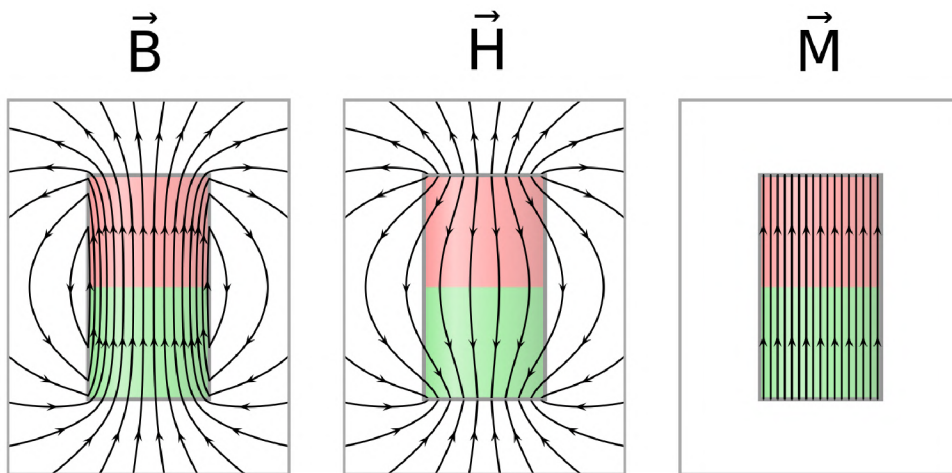


**Figure 1.1.1:** A comparison of magnetic field lines of magnetic flux density  $\vec{B}$ , magnetic field strength  $\vec{H}$  and magnetisation  $\vec{M}$  inside and outside a cylindrical bar magnet [7](edited)

These lines are a kind of analogue to the field lines defined for the electric field. Magnetic induction lines are always closed curves lying in a plane perpendicular to the velocity vector of charge. Unlike the electric field, in the magnetic field, the so-called monopoles exist only in theory, and their existence has not yet been proven.

One way of inducing a magnetic field is through the fact that the movement of electric particles in conductors creates a magnetic field, which is used in electromagnets. Another way of generating the magnetic field comes from the properties of elementary particles, e.g., electrons, which have their own intrinsic magnetic field [1].

While permanent magnets are a source of a magnetostatic field, i.e., a stationary magnetic field, the magnetic field of electromagnets can be dynamically changed by the wiring of the coil. However, as a result of a time-varying magnetic field, many dynamic applications are affected by hysteresis losses [2].

The fundamental quantity defining a magnetic field is magnetic induction (or, in some literature, magnetic flux density)  $\vec{B}$ . The magnetic induction can be defined by the following considerations: A particle charge at rest in a magnetic field is not subject to any force induced by the field. If this particle charge moves through the magnetic field, the field exerts a magnetic force on it. The magnitude of this force depends on the size of the charge and also on the speed and direction of its movement. This force is called the Lorentz force, and the following relationship applies [2]:

$$\vec{F}_L = q[\vec{E} + \vec{v} \times \vec{B}] \quad (1.1)$$

where  $q$  is the observed particle charge,  $\vec{v}$  is the velocity vector of its motion,  $\vec{E}$  is the intensity of the electric field, and finally  $\vec{B}$  is magnetic induction, a fundamental quantity describing the properties of the magnetic field. In cases where no electric field occurs, the (1.1) is solely a magnetic force, and we obtain the following:

$$\vec{F}_L = q[\vec{v} \times \vec{B}]. \quad (1.2)$$

It also follows from the equation (1.1) or (1.2) that if the charge velocity vector is parallel to the magnetic field induction vector, then the Lorentz force is zero. Thereby, the force  $\vec{F}_L$  acting on a charged particle  $q$  moving at velocity  $\vec{v}$  through a magnetic field  $\vec{B}$  is always perpendicular to  $\vec{v}$  and  $\vec{B}$  [1].

*Note:* Magnetic induction is defined by equation (1.1). This equation also fully defines the unit of magnetic induction, the Tesla. A magnetic field has a magnetic induction of 1 T if, when applied to a charge of 1 Coulomb moving at speed 1 m.s<sup>-1</sup> perpendicular to the magnetic induction vector, a Lorentz force of 1 Newton is exerted.

It is important to highlight that Tesla is a rather large unit. In normal engineering applications, the magnitude of the magnetic field is at most measured in units of Tesla. For example, in the air gap of a loudspeaker, the magnetic field strength is usually in the range of 1 or 2 T, and the magnetic field induction produced by magnetic resonance is in the range of 1, 5 to 3 T.

With the use of a cross-product, we can rewrite (1.2) as

$$F_L = |q| v B \sin \varphi \quad (1.3)$$

which confirms that the magnitude of the acting force is zero if and only if  $\vec{v}$  and  $\vec{B}$  are either parallel ( $\varphi = 0^\circ$ ) or antiparallel ( $\varphi = 180^\circ$ ), and the force is at its maximum when  $\vec{v}$  and  $\vec{B}$  are perpendicular to each other.

For the magnetic induction vector, the flux term  $\vec{\Phi}$  for any arbitrary oriented surface  $S$  can be introduced in the following way:

$$\vec{\Phi} = \iint_S \vec{B} dS. \quad (1.4)$$

It is also true that the magnetic flux through any closed surface  $S$  is zero, in other words

$$\oiint_S \vec{B} dS = 0 \quad (1.5)$$

or in differential form

$$\text{div} \vec{B} = \nabla \cdot \vec{B} = 0. \quad (1.6)$$

The magnetic induction can also be expressed in terms of the magnetic potential vector  $\vec{A}$  as

$$\vec{B} = \text{curl} \vec{A} \quad (1.7)$$

and according to [2], it is always possible to choose the vector potential  $\vec{A}$  such that the so-called calibration condition

$$\text{div} \vec{A} = 0 \quad (1.8)$$

is met in the magnetostatic field<sup>1</sup>. With the help of Stokes' theorem, the magnetic flux can be expressed in terms of the line integral, as follows:

$$\vec{\Phi} = \iint_S \vec{B} dS = \iint_S \text{curl} \vec{A} dS = \oint_{\ell} \vec{A} d\ell. \quad (1.9)$$

To introduce some of the following terms, it is necessary to define the magnetic dipole. According to [1], magnetic dipoles are the simplest magnetic structures. The equation (1.5), also referred to in the literature as the Gauss' law for magnetic fields, implies that magnetic monopoles do not exist, i.e., one end of the magnet is a so-called source of the field and the other is a sink. By convention, these are referred to as the north pole and the south pole, respectively.

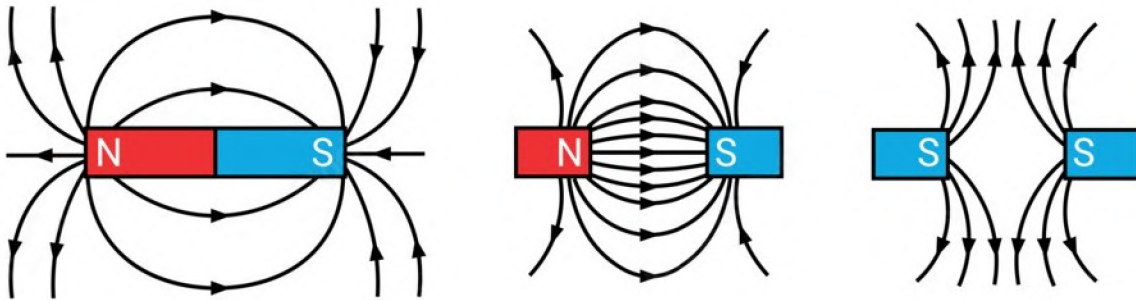


**Figure 1.1.2:** A visualisation of magnetic pole models (from left to right): a magnetic dipole; an attraction of opposite poles; a repulsion of the same poles [8](edited)

<sup>1</sup>For non-stationary magnetic fields, the vector potential can also be introduced, as well as the calibration condition. Since this is not relevant for this work, see [2].

The continuous spatial distribution of magnetic dipoles can be described by the dipole moment density  $\vec{M}$ , i.e., the magnetisation vector. Its proportionality to the similar term of the magnetic polarisation vector  $\vec{P}$  can be formulated as

$$\vec{P} = \mu_0 \vec{M} \quad (1.10)$$

where  $\mu_0 = 4\pi \cdot 10^{-7}$  [H·m<sup>-1</sup>] is the vacuum's permeability. To further describe the magnetic field, a quantity of magnetic field intensity (or magnetic field strength) is also introduced

$$\oint_{\ell} \vec{H} d\ell = \mu_0 I, \quad (1.11)$$

or in differential form with the use of Stokes' theorem

$$\text{curl} \vec{H} = \vec{j} \quad (1.12)$$

where  $I$  is a current and  $\vec{j}$  is the free volume current density at a given point. A way of expressing the magnetic field intensity in terms of magnetic induction is

$$\vec{H} = \frac{\vec{B}}{\mu_0} \quad (1.13)$$

and if for any point in the case of a magnetostatic field, the following is satisfied:

$$\text{div} \vec{B} = 0 \quad (1.14)$$

$$\text{div} \vec{H} = 0. \quad (1.15)$$

Such field is then potential and is describable by a scalar potential  $\phi$ . Another expression for the magnetic field intensity is

$$\vec{M} = \chi_m \vec{H} \quad (1.16)$$

where  $\chi_m$  is magnetic susceptibility, which is a quantity that determines the proportionality between magnetisation and magnetic pole in a substance [3]. Its relation to the permeability  $\mu$  and its dimensionless form, the relative permeability  $\mu_r$ , is described by the following equations:

$$\mu = \mu_0 \mu_r \quad (1.17)$$

$$\mu_r = 1 + \chi_m. \quad (1.18)$$

Based on equations (1.13), (1.17) and (1.18) we can state the following [2]:

$$\vec{B} = \mu_0 (\vec{M} + \vec{H}) \quad (1.19)$$

## 1.2 Magnetic Materials

Magnetic susceptibility is the degree to which a material is magnetised depending on the applied field. On the basis of magnetic susceptibility, the behaviour of magnetic materials can be categorised into antiferromagnetic, diamagnetic, ferromagnetic, ferrimagnetic, and paramagnetic.

Another way of categorising magnetic materials is by their relative permeability  $\mu_r$ , which is the ratio of the permeability  $\mu$  of a magnetic material to the permeability of a vacuum  $\mu_0$ . The relative permeability value is determined by the properties of the atoms that make up the substance.

The individual electrons in the atoms move in small closed loops and generate elementary magnetic fields, which combine to form the resulting magnetic field of the atom. Depending on the arrangement of the electrons in the atom, the magnetic fields inside the atom may cancel each other out completely (see diamagnetic materials) or only partially (paramagnetic materials). This explains the existence of the following groups of magnetic materials [4] summarised in Figure 1.2.1.

### DIAMAGNETIC MATERIALS

Diamagnetism is characterised by the fact that it slightly weakens the magnetic field, i.e., diamagnetic materials exhibit a very small negative magnetisation. They consist of atoms with almost no net magnetic moment[2],[5]. The relative permeability of diamagnetic materials is slightly less than one ( $\mu_r < 1$ ) while reacting to the external magnetic field. Examples of diamagnetic materials are noble gases, gold, copper, mercury, etc. For example, the relative permeability of copper is  $\mu_r = 0,999990$ .

### PARAMAGNETIC MATERIALS

A paramagnetic material can be considered somewhat of a contradiction to the diamagnetic material as its relative permeability is slightly greater than one ( $\mu_r > 1$ ) while exposed to the external magnetic field, thus having no net magnetisation. This means that they slightly amplify the magnetic field [2]. An example of paramagnetic materials is, e.g., sodium, potassium, and aluminium. For example, the relative permeability of aluminium is  $\mu_r = 1,000023$ .

At room temperature, where the magnetic field of diamagnetic and paramagnetic materials is very weak, both types of materials show no hysteresis (see Subsection 1.3).

### FERROMAGNETIC MATERIALS

Ferromagnetic material is characterised by a high magnetic permeability ( $\mu \gg 1$ ), which allows it to become highly magnetic. It also has the ability to retain a permanent magnetic moment. Its elementary magnetic dipoles within the domains are all parallel to each other, see Figure 1.2.1. For example, the relative permeability of steel is  $\mu_r \approx 8000$ .

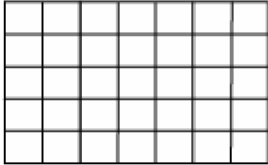
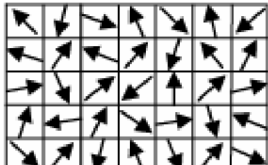
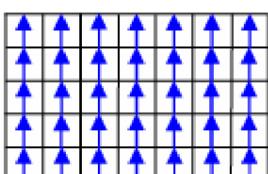
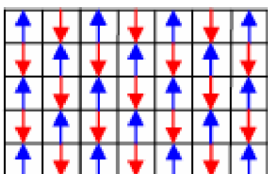
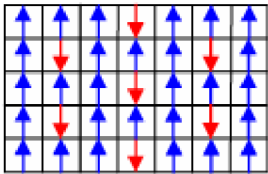
For any ferromagnetic substance, there is a certain temperature above which the substance loses its ferromagnetic properties and becomes paramagnetic. This temperature is known as the Curie temperature. For example, iron has a Curie temperature of  $770^\circ\text{C}$  [4].

### ANTIFERROMAGNETIC MATERIALS

These are nonmagnetic materials with all domains oriented anti-parallel to each other.

## FERRIMAGNETIC MATERIALS

A material is considered ferrimagnetic if only a certain number of domains are oriented anti-parallel.

Type of Magnetism	Magnetic Behaviour	Magnetic Susceptibility	Examples
Diamagnetic		Small and negative	Copper, silver, gold and alumina
Paramagnetic		Small and positive	Aluminium, titanium and alloys of copper
Ferromagnetic		Very large and positive, function of applied field, microstructure dependent	Iron, nickel and cobalt
Anti-ferromagnetic		Small and positive	Manganese, chromium, MnO and NiO
Ferrimagnetic		Large and positive, function of applied field, microstructure dependent	Ferrites

**Figure 1.2.1:** Different types of magnetic behaviour [5]

The cause of magnetisation is the action of exchange forces between neighbouring atoms. Because of these forces, even in the absence of any external action, there is a consensual arrangement of the magnetic fields of the atoms in a small region of the substance. During this spontaneous magnetisation, microscopic regions of  $10^{-3} \text{ mm}^3$  to  $10 \text{ mm}^3$  volume called magnetic domains are formed in the material. However, the individual domains are randomly oriented. Under the influence of an external magnetic field, these domains become aligned, and the material takes on the properties of a magnet. During this process, the volume of the domains gradually increases until they are aligned and the domain structure disappears. We say that the substance is magnetically saturated [4].



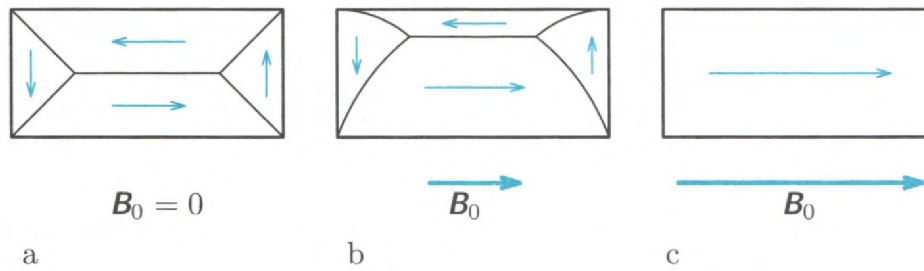


**Figure 1.2.2:** Domain structure of magnetic substance [4]

### 1.3 Magnetic Hysteresis

Hysteresis is the property of a system that does not immediately follow applied influences. Instead, depending on its immediate history, the system's response may be slow or may not completely return to its original point of origin [5].

Magnetic hysteresis is the non-linear dependence of the magnetisation vector  $\vec{M}$  on the magnetic field intensity  $\vec{H}$  shown in the following figure. It is caused by local rotations of the magnetisation vector in the presence of an external magnetic field. This dependence is referred to as a hysteresis curve or hysteresis loop. The curve of the prime magnetisation starting from

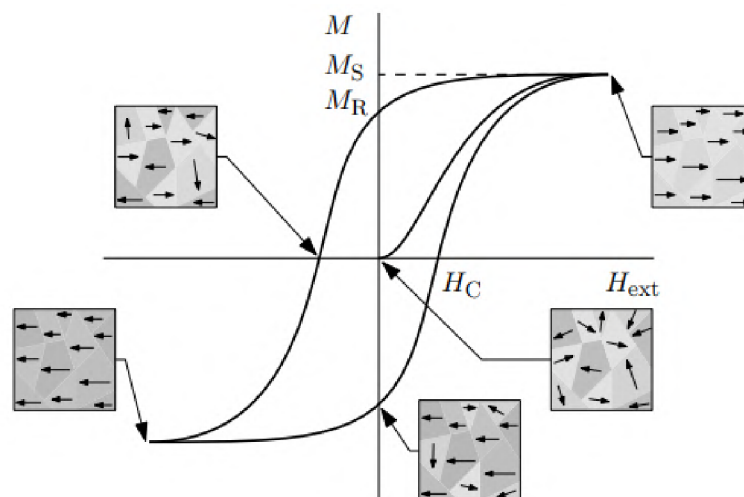


**Figure 1.3.1:** The hysteresis curve [3]

the origin of the coordinate system, i.e., in the absence of the magnetic field, shows the rotation of the magnetisation in the substance in the direction of the increasing magnetic intensity. This maximum attainable value of magnetisation is called saturation magnetisation  $M_S$ . When the intensity of the external magnetic field is reduced, the decreasing magnetisation does not return to its initial point. Instead, it retains a non-zero value when the field is removed, called remanent magnetisation  $M_R$ .

To reverse the magnetisation vector in the opposite direction, an additional field in the opposite direction must be applied. The coercive field  $H_C$  is the magnetic field required to reorient exactly half of the magnetic moments and thus cancel the total magnetisation of the material [3].

In some literature, magnetic hysteresis is presented as the dependence of magnetic induction

on magnetic field strength, in which case we speak of so-called BH curves. The shape and size of the hysteresis loop differ for hard and soft magnetic materials. If the material is easily magnetised, the loop will be narrow, and vice versa. The height of the loop depends on the material's magnetic saturation value, see the following Figure 1.3.2 and the following Table 1.3.1 [5].

Magnetic Property	Soft Magnetic Material	Hard Magnetic Material
Hysteresis loop	Narrow	Large area
Remanence	High	High
Coercivity	Low	High
Saturation flux density	High	Good

**Table 1.3.1:** Brief overview of magnetic properties between hard and soft magnetic materials [5]

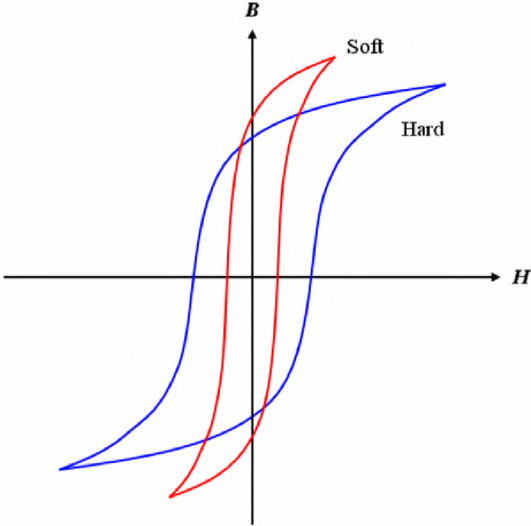


**Figure 1.3.2:** Hysteresis curve for hard and soft magnetic materials [5]

An example of soft magnetic material is a temporary magnet or electromagnet, which is made from soft iron. On the other hand, permanent magnets made from hard magnetic materials such as steel, cobalt steel, or carbon steel are hard magnetic materials.

# Chapter 2

## Magnetically Active Liquids

This chapter offers a comprehensive introduction to magnetically active liquids. It provides an overview of both ferromagnetic and magnetorheological liquids, along with a handful of manufacturers. This chapter draws mainly upon the following sources: [5], [9], [10], [11],[12], [13], [14].

As explained in detail in the previous chapter, only a handful of metals possess magnetic properties. The observed phenomenon of ferromagnetism can be attributed to the alignment of the tiny magnetic moments of individual atoms. However, this phenomenon can only be observed in the solid state of matter. Nevertheless, it is worth noting that a particular class of material does exist whose properties consist of fine ferromagnetic particles suspended in a carrier fluid. This combination of magnetism and the fluid state of matter, as described in [15], gives rise to unique and remarkable properties.

In nowadays' terminology, these so-called smart fluids are suspensions known as magnetic liquids, which can be further divided into two types based on the average size of their magnetic particles: ferromagnetic liquids (Section 2.3) and magnetorheological liquids (Section 2.4)<sup>123</sup>. To study these liquids, new fields had to be introduced, as classical hydrodynamics does not deal with the effects of the magnetic field or electricity. A science field that studies the interaction between a magnetic field and a magnetically polarizable, electrically non-conducting liquid is called ferrohydrodynamics (FHD). Other fields, based on the properties they study, include electrohydrodynamics (EHD), which examines the force interactions between an electric field and an electrically polarizable liquid, i.e., electrorheological liquid (ER)<sup>4</sup>, and magnetohydrodynamics (MHD), which studies the interaction between a magnetic field and a magnetically polarizable, electrically conductive liquid [11], [17].

The alteration of properties in the presence of an external magnetic field can be achieved by permanent magnets and electromagnets, which is known as the magnetorheological, or magnetoviscous, effect. In order for the use of magnetically active liquids to be effective, it is crucial that the effect is reversible and that the properties of the liquid revert to their original

---

<sup>1</sup>Another so-called bimodal magnetic liquid is presented in [16] with magnetic particles dispersed in a magnetically active carrier liquid.

<sup>2</sup>In some works, it is possible to see terms such as ferrofluid (FF) and magnetorheological fluid (MRF) that are employed to refer to ferromagnetic and magnetorheological liquids, respectively. These terms are also used in this work without any loss of meaning, as it is well established that all liquids are also fluids, but not vice versa.

<sup>3</sup>Unfortunately, the nomenclature of magnetic fluids is not entirely strictly adhered to. Some authors refer to ferromagnetic liquids as a superordinate term, including both MR liquids and liquids with smaller particles. Others specifically refer to them as magnetic nanofluids (MNFs).

<sup>4</sup>Liquids that, when an external electric field is applied to the liquid, isolate particles from each other, causing them to form a chain-like structure similar to magnetorheological fluids [12].

state when the external magnetic field is removed. Consequently, low remanence and coercivity requirements are placed on the particles, which ensures that each repeated application of a given magnetic field under the same conditions will result in the same change in properties with each application.

## **2.1 Composition of Magnetically Active Liquids**

The composition of magnetically active liquids is comprised of three distinct parts.

### **MAGNETIC PARTICLES**

These are mediators of magnetic interaction, with dimensions in the order of nanometers or micrometres for ferromagnetic liquids and magnetorheological liquids, respectively. In many cases, they are a compound of iron with another element, for instance,  $\text{Fe}_3\text{O}_4$ . Additionally, alloys are employed, such as the iron-cobalt alloy to powdered iron, due to their high magnetic saturation value [13].

### **CARRIER LIQUID**

The carrier liquid is a medium in which the magnetic particles are dispersed. Usually silicone, synthetic, mineral oils, and even water are used, and the addition of additives effects the polarizability of the particles and improves stabilisation [18].

The carrier fluid exerts a profound influence on the final properties of the magnetic fluid, both in the activated and unactivated states. The viscosity of the magnetic fluid in its unactivated state is determined by the carrier fluid, as is the resulting density. Furthermore, the operating temperature range is influenced by the choice of carrier fluid [13].

### **SURFACTANT**

Surfactant is a coating agent on the particle surface employed to prevent the agglomeration and sedimentation of the particles. The desired effect is achieved when the hydrophilic end of the chain is fixed and bonded to the surface of the particle, while the other hydrophobic end is attracted to the surrounding fluid and repelled by the chain end of the surrounding particle. The particles with the same charge repel each other in the liquid and thus do not combine into larger units, which could result in a reduction or complete suppression of the magnetorheological phenomenon. This negatively affects the magnetic saturation value of the liquid. An example of a surfactant is oleic acid [13], [9].

Apart from these three components, other additives can be employed. These include agents that modify the pH of the carrier liquid and antioxidants that enhance the resistance and durability of the particles to, e.g., thermal influence [13].

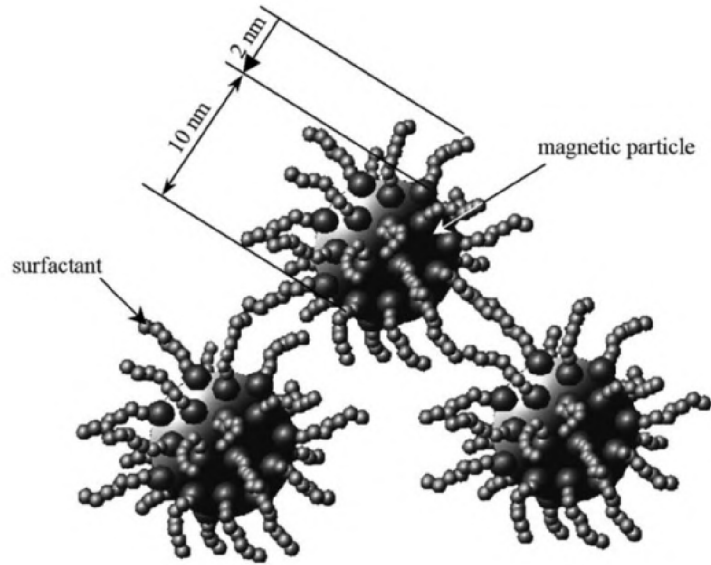


**Figure 2.1.1:** Schematic of magnetic particles with surfactant (purposefully not in scale for clarity) [9]

## 2.2 Magnetorheological and Magnetoviscous Effect

The magnetic field exerts a profound influence on the particles in the liquid, inducing the formation of chain-like structures that bear resemblance to magnetic field lines. This process results in a notable increase in viscosity, accompanied by the emergence of a yield stress below which the liquid assumes the characteristics of a solid. The viscosity and yield stress values are dependent on the strength of the magnetic field. These properties increase with higher field strength.

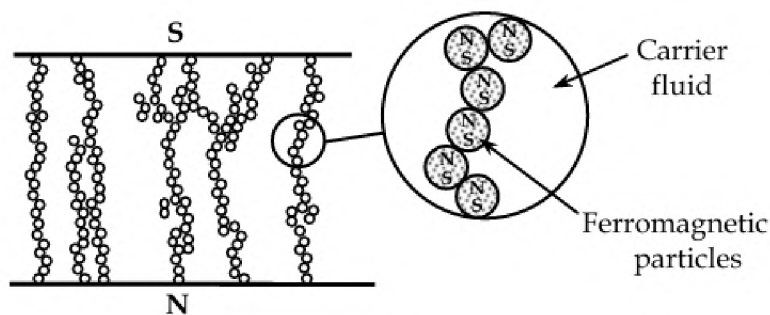


**Figure 2.2.1:** A Schematic of the described effects [19]

In the case of ferrofluids, we speak of the magnetoviscous effect because their internal friction and, therefore, viscosity change with the intensity of the magnetic field applied. In contrast to magnetorheological liquids, which undergo a transition to a solid state under the application of a magnetic field, ferromagnetic liquids remain liquid even at higher magnetic field strengths applied [9].

## 2.3 Ferromagnetic Liquids

Ferrofluids are colloidal suspensions with particle dimensions of several nanometers. Due to the size of the particles, Brownian motion, which is the random movement of particles dispersed in a liquid or gas, has a significant effect on the particle settling problem, along with van der Waals and magnetic forces. Furthermore, each particle forms a so-called Weiss domain and has its own magnetic moment, which is characteristic of single-domain particles. In a single-domain particle, all the atoms of the particle have their magnetic moment aligned in one direction, cooperating with each other (similarly as in Figure 1.2.1). This results in an externally manifested enormous magnetic moment [20].

Unlike magnetorheological fluids (Section 2.4), ferrofluids do not have a proven yield strength [12]. Their different magnetic behaviour is also a consequence of the small particle size, where these single-domain particles present in the liquid are superparamagnetic<sup>5</sup>. The mathematical description of magnetic liquids is generally not a simple matter, and certainly not in the case of ferromagnetic liquids, since the behaviour of each individual particle must be taken into account due to single-domain behaviour.

For example, the change in viscosity of a magnetically active liquid depends not only on the strength of the magnetic field but also on its orientation with respect to the direction of flow. The magnetic field tends to align particles according to the induction lines. If the particle is oriented so that the velocity vortex vector is parallel to the magnetic field, there is no magnetoviscous effect. However, if the vector is perpendicular to the direction of the strength magnetic field, a torque is produced that prevents the particle from rotating freely. This has the effect of an increase in the apparent viscosity of the liquid. The angle between the velocity vortex vector and the magnetic field is responsible for the anisotropic behaviour of the liquid [10].

## 2.4 Magnetorheological Liquids

The magnetorheological liquids display a significant and reversible change in their rheological properties (elasticity, plasticity, or even viscosity). The description of the behaviour of magnetorheological fluids can be based on the description of ferromagnetic liquids, with the following differences:

- The magnetorheological effect plays a key role in the liquid's behaviour.
- Particles in magnetorheological fluid are no longer single-domain.
- The energy of Brownian motion is negligible.

The particles of the magnetorheological liquid are therefore multidomain, exhibit dipole behaviour only when a magnetic field is applied, and, therefore, react differently compared to ferrofluids under the same influence of the magnetic field. Magnetorheological liquids can change their viscosity with the formation of a chain structure and solidify when a magnetic field is applied, whereas ferromagnetic liquids retain their liquid form. When subjected to the magnetic field, the particles are oriented along the direction of the applied magnetic field. These particles are assembled into a uniform polarity and connected to the walls. Upon alignment, iron particles remain stationary within their respective flux lines, acting as a barrier to external forces.

---

<sup>5</sup>A property characterised by a high degree of magnetisation in the presence of weak and medium magnetic fields, in contrast to paramagnetic substances [11].

In this context, yield stress represents the maximum stress-strain relationship. When the stress reaches maximum, the chains will break, allowing the fluid to flow even if the magnetic field is still applied [5].

### 2.4.1 Rheology of Magnetorheological Liquid

Rheology is the study of the relationship between shear stress  $\tau$  and shear strain  $\dot{\gamma}$ . A rheological model enables the mathematical description of the mechanical behaviour of the continuum in the presence of an external load.

The carrier liquid is typically Newtonian in its behaviour. However, when considered as a whole, it exhibits non-Newtonian behaviour. A plethora of models have been developed to describe the behaviour of magnetorheological liquids, see [21]. One of them is the Herschel-Bulkley model and its special case for  $n = 1$ , the Bingham model, as follows, respectively:

$$\tau = \tau_y(\vec{H})\text{sgn}(\dot{\gamma}) + \mu \dot{\gamma}^n \quad (2.1)$$

and for  $n = 1$ :

$$\tau = \tau_y(\vec{H})\text{sgn}(\dot{\gamma}) + \mu \dot{\gamma} \quad (2.2)$$

where  $\tau_y$  is the yield stress dependent on the strength of the magnetic field. The yield stress is defined as the shear stress required to initiate flow, and it is evident that the equations hold true iff  $\tau \geq \tau_y$ .

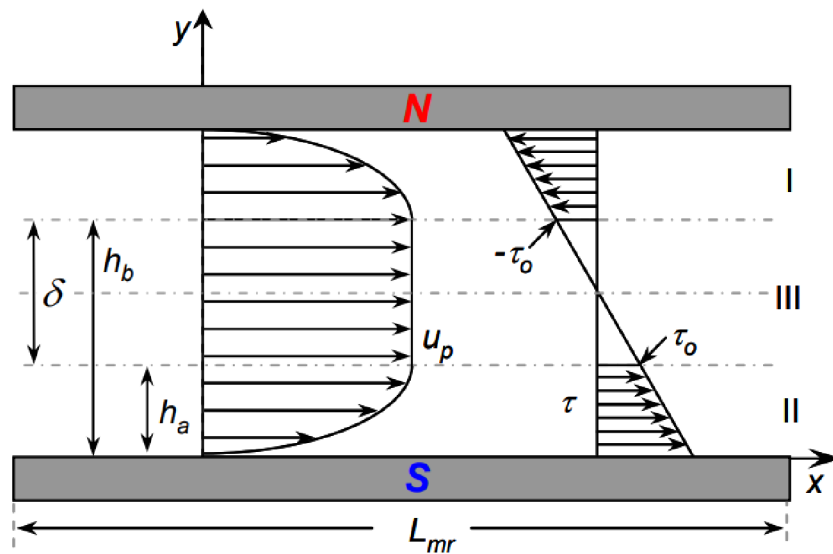


**Figure 2.4.1:** Fluid flow of magnetorheological liquid through fixed parallel plates [14]

From the figure, it can be seen that the shear stress  $\tau$  increases linearly with decreasing distance from the magnet pole. The value of the shear stress in regions I and II is called the post-yield region. It exceeds the yield stress value and, therefore, the fluid flows. In region III, i.e., pre-yield region, the shear stress is below the critical value and the fluid behaves more like a solid body.

In the majority of engineering applications, the Bingham model represents an effective tool for describing the fundamental characteristics of magnetorheological liquids. However, the question, of to what extent it can be considered universally valid persists. It is evident that the

characteristics of magnetic liquids, generally, can vary considerably, particularly in terms of particle size, concentration, chemical composition, and carrier fluid, which makes it challenging to assume that the Bingham model is, in general, feasible [22], [23]. In addition to the Bingham model, other approaches can be found, for example, in [24].

### 2.4.2 Modes of Operation

In general, magnetorheological liquid devices operate according to one of the following modes of operation, or a combination of these modes, depending on the function of the system. These modes are known as valve mode, shear mode, squeeze mode, and gradient pinch mode. Prior to the design of any magnetorheological liquid device, it is essential to consider the rheological and magnetic properties, the circuit, and the working mode of the magnetorheological liquid. This part draws from [5].

#### VALVE MODE

In the valve mode, in some literature flow mode, the fluid is situated within the space between the fixed plates. The pressure drop between the ends creates a fluid flow from one end to the other.

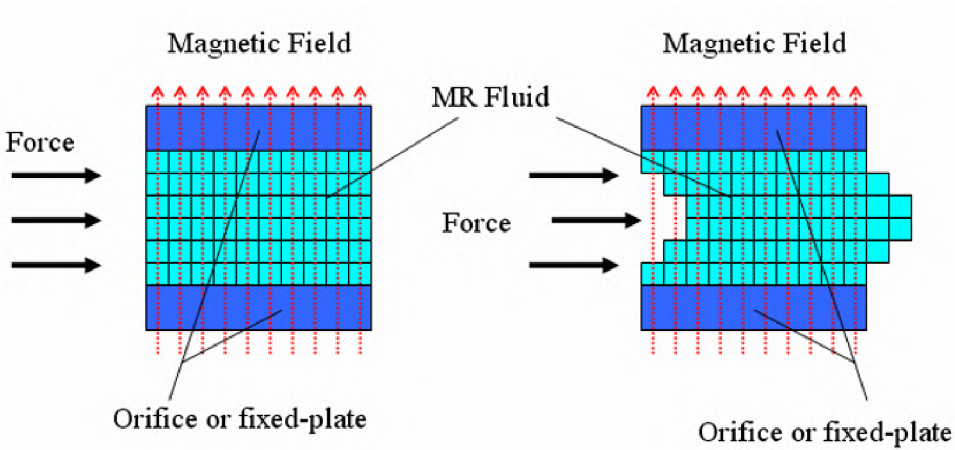


Figure 2.4.2: Schematic of valve mode [5]

The magnetic field applied perpendicular to the direction of the flow is employed to alter the viscosity of the magnetorheological liquid in order to regulate the flow. As a consequence, an increase in yield stress or viscosity modifies the velocity profile of the fluid in the gap between two plates, see Figure 2.4.1 [5].



## SHEAR MODE

In the case of shear mode, one plate moves in a parallel direction to the other either by sliding or rotating. In the unactivated state, the magnetic liquid is observed to move between the plates in the direction indicated in the following figure. The viscosity of the liquid increases with the magnetic field applied perpendicularly, which consequently leads to an increase in the resistance to the plate movement.

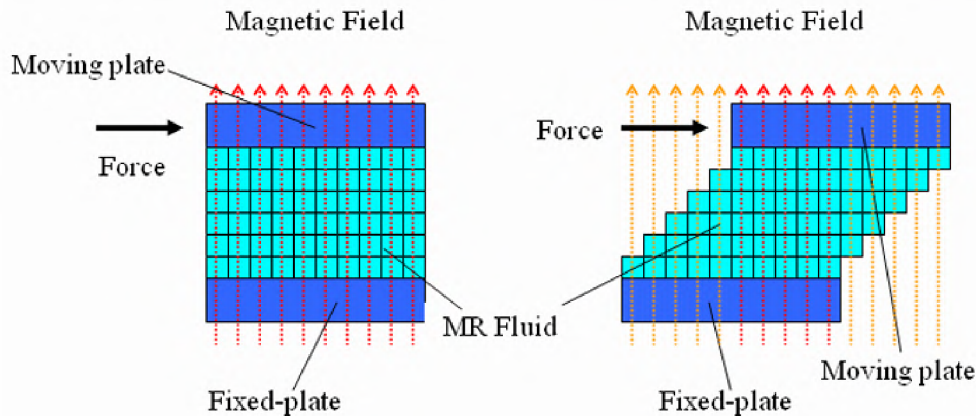


**Figure 2.4.3:** Schematic of shear mode [5]

## SQUEEZE MODE

The third, squeeze mode, has not been widely investigated. This mode operates under the application of a force in the direction of a magnetic field, which results in a reduction or expansion of the distance between the parallel plates.

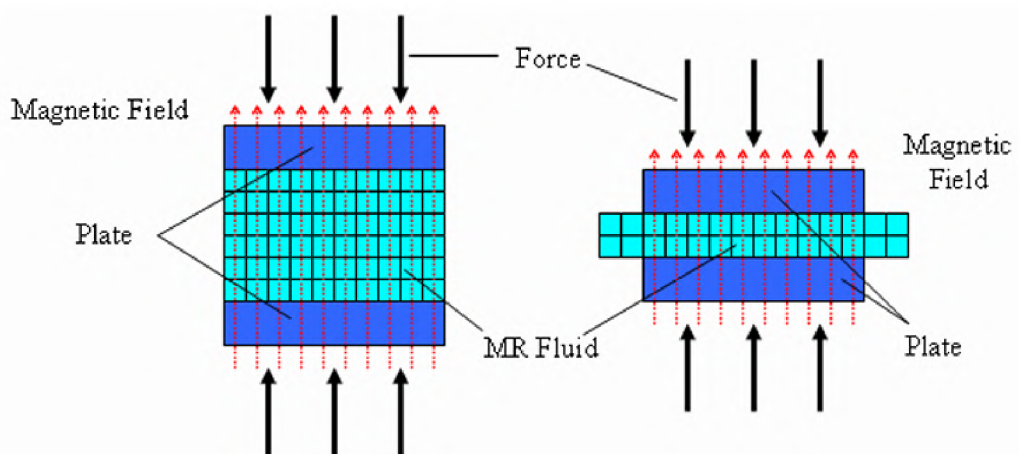


**Figure 2.4.4:** Schematic of squeeze mode [5]

In this mode, the magnetorheological liquid is subjected to a dynamic (tension-compression alternation) or static (individual tension or compression) load. As the magnetic field charges

the particles, the particle chains formed between the walls become rigid with rapid changes in viscosity. The displacements involved in squeezing mode are in the range of millimetres but require large forces.

#### GRADIENT PINCH MODE

In contrast to the aforementioned modes, the gradient pinch mode employs a different approach, and today it is the least studied. The magnetic field within the flow channel is oriented to activate the fluid in these areas, resulting in the generation of high yield stresses in these regions and the establishment of low yield stresses in the central zone. This yield stress distribution is non-uniform [25], [26].

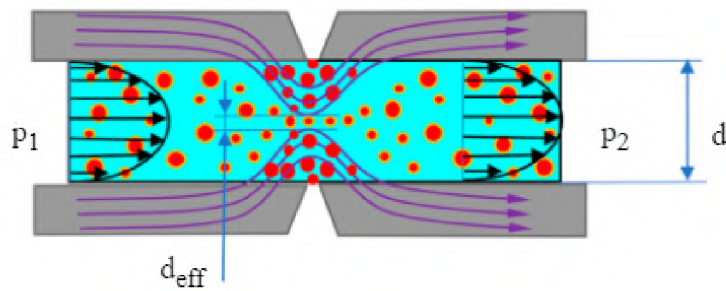


**Figure 2.4.5:** Schematic of shear mode [27]

Consequently, as can be seen in Figure 2.4.5, a Venturi-like contraction is formed exclusively through the action of the material itself, without any alteration to the flow path geometry.

# Chapter 3

## Matter of Scale

### 3.1 Microfluidics

Microfluidics can be defined as either a scientific discipline that studies the behaviour of fluids at the micro- to nanometer scale or as a technology for fabricating microfluidic devices containing channels and chambers through which fluids flow.

The fundamental principle of microfluidic technology is the integration of a complex system into a simple microfluidic system that would otherwise require an entire laboratory. The ability to work at this scale offers several advantages, including the ability to analyse samples with greater accuracy at the point of introduction and to conduct faster reactions due to the specific fluid dynamics involved. This results in a significant reduction in chemical waste.

A typical microfluidic device is a microfluidic chip, which is a network of microchannels etched or moulded into a material such as glass, silicon, or polydimethylsiloxane (PDMS). The design of the network of microchannels is meticulously engineered to align with the specific requirements of the chip, encompassing a range of applications such as lab-on-a-chip (LoC), pathogen detection, electrophoresis, DNA analysis, and more.

At both ends of the microchannels, there are holes punched through the chip, representing inputs and outputs. Fluids are injected and drained from the microfluidic chip via, e.g., attached tubing or syringe adapters.

These elements can be embedded either inside the chip in the form of different valves or outside the chip. In the case of external active systems, pressure regulators, injection pumps, or peristaltic pumps are used. In a passive way, hydrostatics can be used to control flow pressure [28], [29], [30].

From a scientific perspective, microfluidics is a subfield of fluid mechanics. However, as the name suggests, the length scales in microfluidic systems are significantly smaller than in classical fluid mechanics, resulting in different fluid physics behaviours [31].

In microfluidic systems, capillary and surface tension forces exert a dominant influence over gravitational forces. The dominance of capillary forces is responsible for the laminar flow. It can be demonstrated that turbulent fluid flow is not possible in microfluidic systems. This fact renders it relatively straightforward to predict the behaviour of the fluid. The mixing of two fluids occurs exclusively via diffusion [32], [33]. This chapter draws from the following sources: [28] -[34].

## REYNOLDS NUMBER

The dimensionless Reynolds number  $Re$  is used to describe whether the fluid is flowing laminarly or turbulently. The critical value of the Reynolds number at which the transition from one type of flow to the other occurs is important. In general, values below 2300 are considered to be laminar flow. Values greater than 2300 indicate turbulent flow (in the case of a fully flowing circular pipe). The formula to calculate the Reynolds number is

$$Re = \frac{\rho d \vec{v}}{\eta} \quad (3.1)$$

where  $\rho$  is the fluid density,  $d$  is characteristic dimension (often the diameter of the pipe),  $\vec{v}$  is fluid velocity, and  $\eta$  is dynamic viscosity. In microfluidics,  $Re$  is in the order of units, up to hundreds at most, therefore, only laminar flow is considered. It is also called streamline flow because it is characterised by non-intersecting streamlines. The fluid moves smoothly in layers. It is stationary when in contact with a horizontal surface, but all the other layers slide over each other [35]. Other relations, such as Hagen-Poiseuille equation, Péclet number, Capillary number, Bond number and many others are also employed to describe the behaviour of a liquid on a microscopic scale.

It is important to note that in the context of microfluidics, the no-slip condition is typically applied to the wall. This condition implies that the fluid in contact with the wall moves at the same velocity as the wall itself. However, this is not always the case in microfluidics due to the small size of the system [36].

## 3.2 Millifluidics

Millifluidics involves the manipulation and observation of fluids in channels in the range of a few millimetres with similar techniques and principles as microfluidics. And although millifluidics uses a larger amount of fluid than microfluidics, it is still a minimal amount compared to macrofluidic methods. Millifluidic channels can often achieve the same level of fluid mixing as microfluidic channels, depending on the specific case requirements. Millifluidics offers many of the same advantages as microfluidics, but millifluidic chips are often easier and cheaper to manufacture [37].

## 3.3 Micromagnetofluidics

Micromagnetofluidics is an interdisciplinary field that combines the principles of microfluidics, magnetohydrodynamics and magnetism to manipulate and control magnetically active liquids at the microscopic level. This field uses magnetic fields to influence the behaviour of liquids containing magnetic particles, allowing precise control and manipulation of these liquids in microfluidic systems.

One of the key benefits of micromagnetofluidics, is its high accuracy and control. The ability to use magnetic fields to manipulate fluids allows very precise control over the movement and mixing of fluids, which is essential for many applications in biotechnology and chemistry. Micromagnetofluidics is therefore a powerful and versatile approach to manipulating fluids at the microscopic level, with a wide range of applications in science, technology, and medicine. The field of micromagnetofluidics and its subfields can be visualised by the Figure 3.3.1.

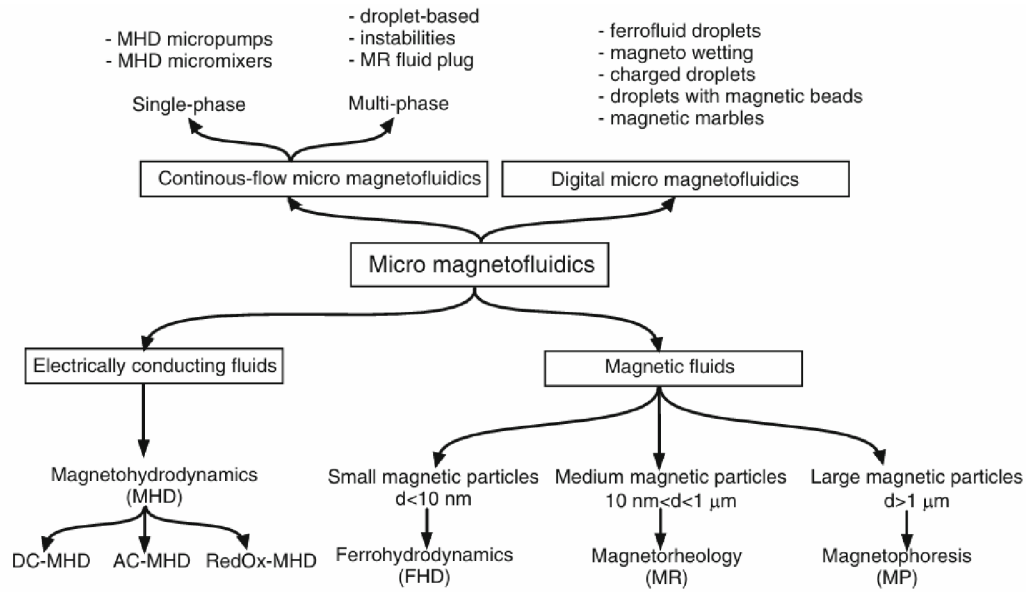


**Figure 3.3.1:** Micromagnetofluidics, its subfields and representative applications [34]

### 3.4 Clarification

While designing the experiment, it was suggested that it would be better to work with milifluidics instead of microfluidics for the following reasons:

- From an economic and logistical point of view, it was quite a challenge to find a supplier who could provide glass tubes of such a small diameter in small quantities, e.g., 3-5 pieces for each diameter.
- From a practical point of view, magnetorheological liquid was chosen as an appropriate medium for our experiment because:
  - a) From the properties of both types of liquids, it is evident that if we were to choose the ferrofluid, no pressure difference would occur, and if so, it would be negligible. Furthermore, at the present state of the art, neither the modes of operation nor the existence of yield stress have been proven.
  - a) However, if we were able to obtain such delicate glass with diameters in the micrometre range, we could face the problem that the magnetorheological liquid would not fit into the tubes due to the size of the particles.

Thus, taking into account the aforementioned arguments, we decided to choose the safer option. Nevertheless, we opted for the smallest available diameters of the glass tubes available. The arguments are summarised in the following table:

	$\varnothing[\mu\text{m}]$	$\varnothing[\text{mm}]$
FF	Little to no pressure detectable	Little to no pressure detectable
MRF	Liquid would not fit	Safe configuration

**Table 3.4.1:** An overview of the arguments

# Chapter 4

## Applications

### 4.1 Lab-on-a-Chip, Microfluidic Devices and Applications

A lab-on-a-chip is a microfluidic platform that integrates various laboratory operations, including biochemical analysis, chemical synthesis, and DNA sequencing. Consequently, lab-on-a-chip devices are not merely a collection of microchannels; rather, they comprise integrated pumps, electrodes, valves, electrical fields, and electronics. Currently, various flow control instruments can be employed to construct a comprehensive lab-on-a-chip system [38].

Microfluidic devices, in general, are used for their major advantages, mainly the small size of the device and the need for a small sample for analysis. We will list some of them [36], [28]:

- *Micropumps* are small-scale pumps used to control the flow of liquids within microfluidic systems.
- *Microvalves* are devices used to regulate or stop the flow of fluids in microfluidic channels.
- *Microreactor* are small-scale reactors mainly used for chemical synthesis.
- *Micro-mixers* are essential for applications requiring precise control over mixing ratios and reaction kinetics. The mixing can be done either actively, which is a process that relies on external energy to introduce velocity gradients in the substances being mixed, thereby inducing mixing. Another way of mixing two liquids in microscale is passively, i.e., relying solely on internal energy of the system with the help of appropriate design of the fluid domain (T-junctions and Y-junctions).
- *Organ-on-a-Chip* are advanced microfluidic devices mimicking the structure and function of human organs. They are used mainly for disease modelling and tissue engineering.
- and others, such as *Microfluidic droplet generator, microfluidic sorting device, microfluidic electrophoresis device and microfluidic cell culture device*.

The field of microfluidics has found its use across many fields, namely [30]:

- *Biomedicine*: a so-called lab-on-a-chip make it possible to integrate many medical tests on a single chip.
- *Cell biology research*: because microchannels have the same characteristic size as biological cells. Microfluidic chips allow easy manipulation of individual cells and rapid drug changes.

- *Others*: drug screening, glucose testing, chemical microreactors, electrochemistry, micro-processor cooling or micro fuel cells.

The Figure 4.1.1 shows several concepts of micropumps using ferromagnetic liquid [34].

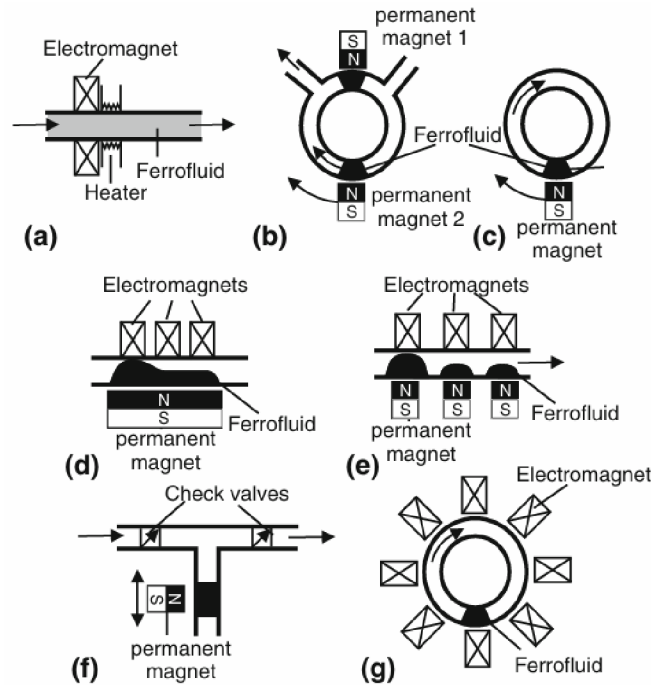


**Figure 4.1.1:** (a) magnetocaloric pump; (b) annular pump with two ferromagnetic liquid pumps; (c) annular pump with one ferromagnetic liquid pump; (d) peristaltic pump; (e) pump with three ferromagnetic liquid valves; (f) pump with check valves and ferromagnetic liquid piston; (g) stepper pump with ferromagnetic liquid [34]

## 4.2 Applications of Magnetically Active Liquids

Here is a list of applications for magnetically active liquids. For discussion on the selection of application see Chapter 4.3.

### BIOMECHANICS AND MEDICINE

- *Therapy* - Targeted medicament transport by means of magnetic liquid hyperthermia [39].
- *Hyperthermia cancer treatment* - By applying a high-frequency alternating magnetic field, the biocompatible nanoparticles of the ferromagnetic liquid are heated and, subsequently killing cancer cells [39].
- *Blood circulation pump seal* - One possible applicable method is, e.g., a ferromagnetic liquid acting as a seal on the shaft of the artificial heart, more on that, see [40], [41], [22].
- *Prosthetic limb replacements* - A design using magnetorheological liquid as a brake or clutch in a knee brace is proposed in [42].

## AUDIO SPEAKERS

Ferromagnetic liquids based on either synthetic hydrocarbons or esters are used for this application [43]. By using a permanent magnet and ferromagnetic liquid, it is possible to dampen vibrations and even dissipate the heat generated. This leads to improved performance and suppression of unwanted audio elements [44].

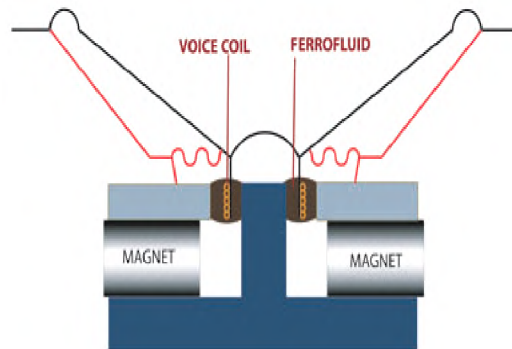


**Figure 4.2.1:** Schematic of an audio speaker with ferromagnetic liquid [43]

## SEALS

Both ferrofluid and magnetorheological fluid can be employed in the manufacture of seals for static and dynamic applications. In contrast to the conventional rubber sealing of shafts, there is no friction between the solid components as the magnetic liquid sealing is based on the contactless principle. For a more detailed study, see [45].

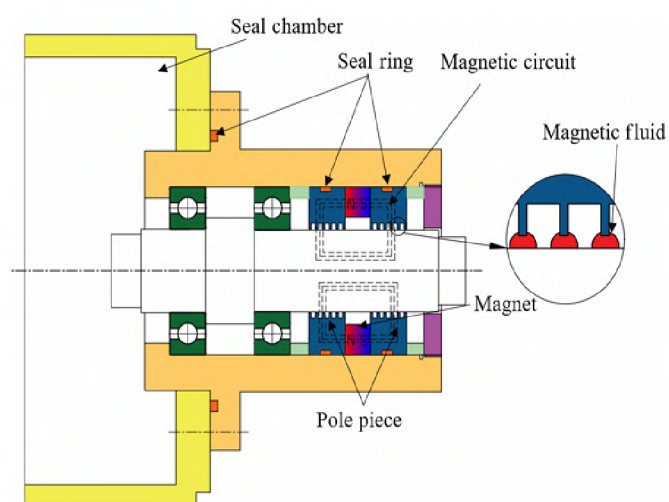


**Figure 4.2.2:** Schematic of the magnetic liquid sealing [45]



## BRAKES

The concept is based on a torque-transmitting disc on a shaft that is surrounded by the magnetorheological liquid, thus serving as a permanent magnet. This part is enclosed by an electromagnet, which, when activated, causes the magnetorheological liquid to expand, filling the space in between both parts, i.e. the shaft or disc and the electromagnet. This then switches on the circuit and causes braking. One advantage is the reaction time and smooth, comfortable deceleration [46], [47].

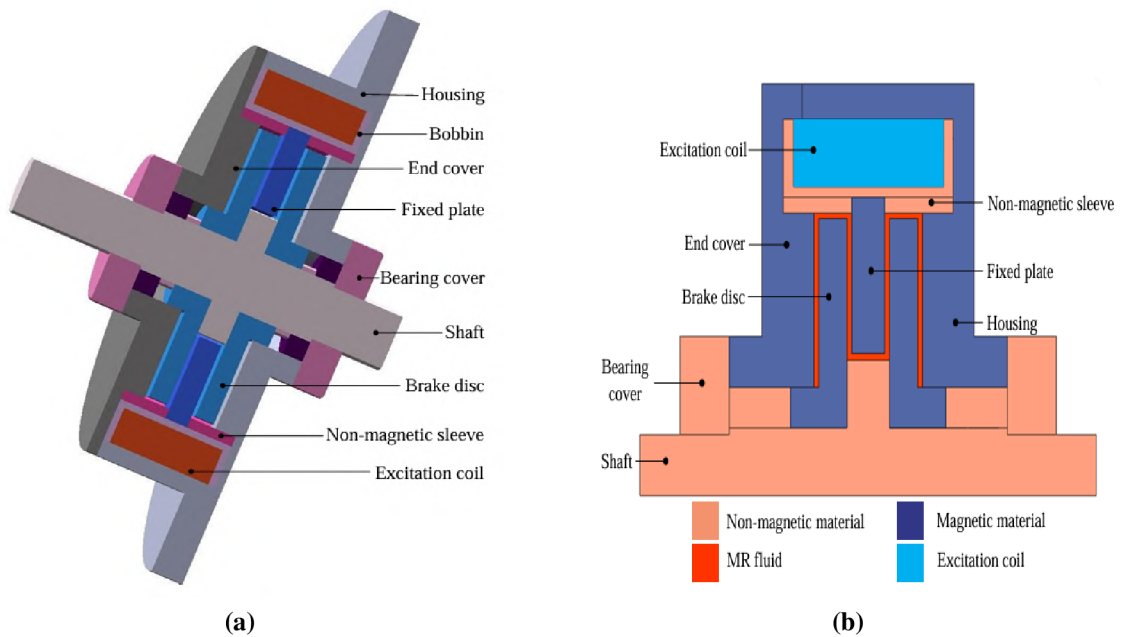


**Figure 4.2.3:** (a) three-dimensional model and (b) material distribution of the MR brake [47]

## FLUIDIC SOFT ROBOTS

These are systems where fluid (liquid or gas) is used to pressurise a soft structure in a controllable way. A great example is shown in [48], where a magnetorheological liquid is used as the working fluid in a system of channels with an inner diameter 1,6 mm. With strategically placed magnetic fields, it is possible to modulate the pressure of the flow to inflate the soft structure, as can be seen in Figure 4.2.4.

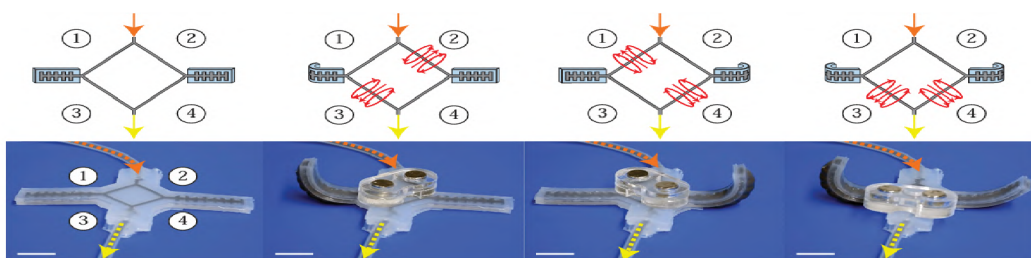


**Figure 4.2.4:** Schematic showing magnetic field placement to independently control the motion of two actuators; the MR fluid is continuously flowing from the top (orange arrow) [48] (edited)

DAMPERS

The principle of dampers with magnetorheological liquid is as follows: if no current is present, then the behaviour is that of a standard damper. On the contrary, if the current and hence a magnetic field pass through the coil, the fluid flow in the radial gap is limited, thus changing the characteristics of the damper. This allows us to have control over the damping and to respond almost instantaneously to the actual damping needs. These dampers find applications in various fields, namely railway technology and the military. For a thorough and detailed description, see [11].

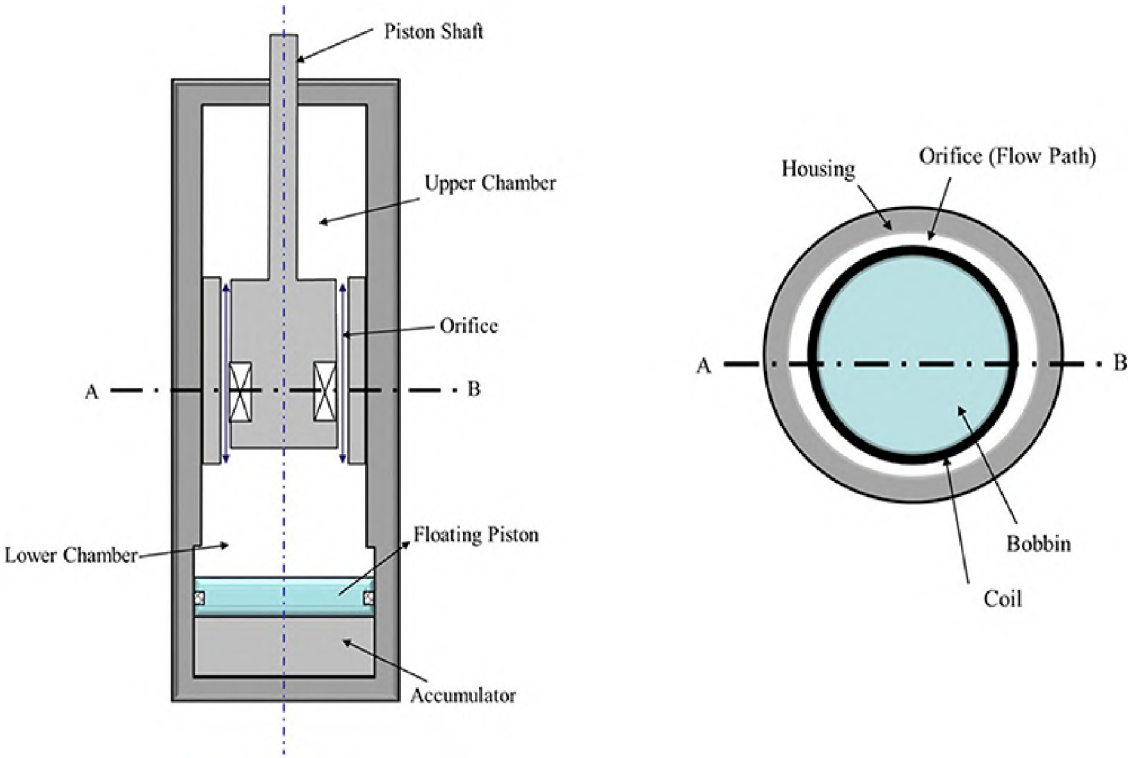


Figure 4.2.5: Schematic of a MR damper [49]

OTHER

Other possible applications include bearings stepper motors, microfluidics, clutches, sink-float separation, machining, construction, or even optics. Magnetically active liquids have become more available in recent years due to their cheaper production.

### 4.3 Lubrication-Induced Instabilities in Journal Bearings

This chapter introduces the selected hydrodynamic device and presents the problem that could be optimised using the knowledge gained in the theoretical part. Hydrodynamic, or journal bearings, are used in a wide range of industries today. This is due to their simplicity of design and durability. The presence of a journal bearing in a mechanism with a rotating shaft can, under certain conditions, lead to the instability of the lubrication film, which is manifested by vibrations and may result in its complete failure, which subsequently damages the bearing. In the case of turbines, this can even have devastating consequences. The ability to predict instabilities based on varying input parameters is crucial for the development of systems equipped with such bearings. Furthermore, a more profound comprehension of the mechanisms that give rise to the erratic behaviour of the lubrication film is also a worthwhile pursuit. Studies have shown that a multitude of parameters have been shown to be involved in the emergence of unstable lubrication behaviour [50], [51], [52], [53].

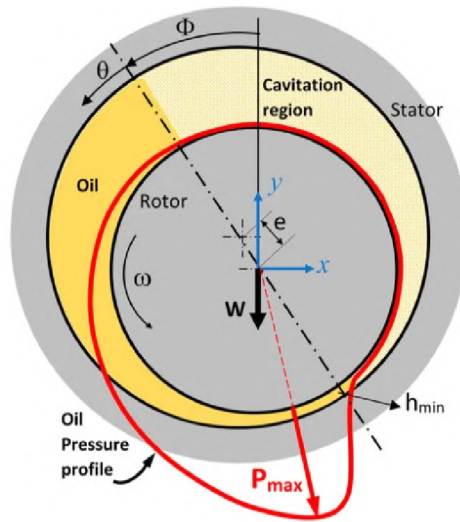


**Figure 4.3.1:** Schematic of journal bearing [54]

While operating, journal bearings primarily employ hydrodynamic lubrication mode, with the exception of the initial start-up and the subsequent running-in period. This operational mode eliminates the potential for material wear.

The hydrodynamic lubrication mode is characterised by the formation of a wedge gap between the journal (rotor) and the housing (stator), see Figure 4.3.1.

The journal draws the lubricant under itself as it rotates, creating a pressure field. The theory of hydrodynamic lubrication is described by the Reynolds equation:

$$\frac{\partial}{\partial x} \left( \frac{h^3}{\eta} \frac{\partial p}{\partial x} \right) + \frac{\partial}{\partial z} \left( \frac{h^3}{\eta} \frac{\partial p}{\partial z} \right) = 6\tilde{U} \frac{\partial h}{\partial x} \quad (4.1)$$

where  $p$ ,  $h$ , and  $\eta$  are the pressure, film thickness, and viscosity of the lubricating fluid respectively, and  $U$  is the relative velocity of bearing surfaces [55].

Additionally, they exhibit a high load capacity, even at high circumferential speeds, and are capable of effectively dampening shock and vibration. Furthermore, their built-up area is relatively small. However, their disadvantage is the lack of load capacity while at rest, but these are not concerns for this work. The instabilities of interest are those related to lubricants,

especially the oil whirl, the oil whip, and the dry whip. All of these instabilities are characterised by the precessional movement of the journal within the clearance of the housing. These will be briefly introduced in the following part [56], [57], more thoroughly in [51].

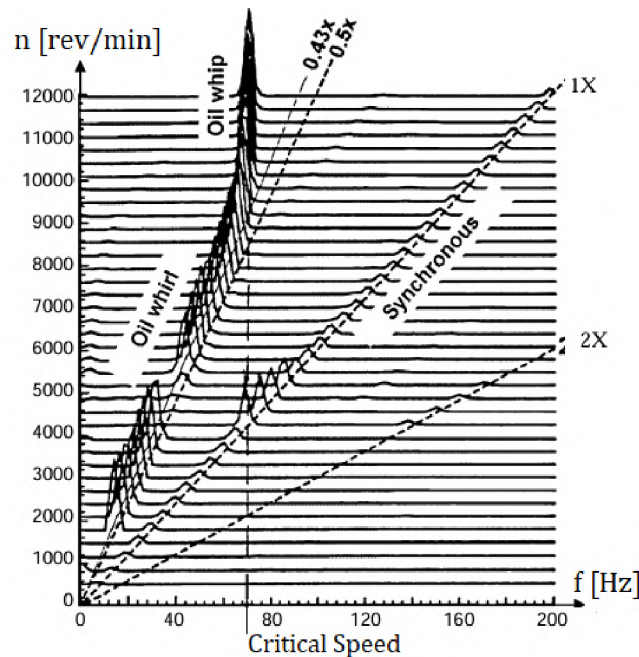


**Figure 4.3.2:** Development of the oil whirl followed by the oil whip [58] (edited)

The progression of these instabilities can be described with the aid of spectral stability analysis, see Figure . The y-axis represents the rotor (machine) speed, the x-axis represents the frequencies of the system vibrations and the z-axis represents the vibration amplitudes [50].

### OIL WHIRL

The oil whirl is form of self-excited chatter and is present usually at 40 percent to 48 percent of journal RPM. However, if vibration aplitudes reach 40 to 50 percent of the bearing clearance, then it is considered severe and corrective actions must be forced [56].

### OIL WHIP

The oil whip occurs when the frequency of the oil whirl coincides and becomes locked with system's natural frequency. If left untouched, oil whip may cause destructive vibration leading to a catastrophic failure in a short matter of time [56].

### DRY WHIP

This instability arises in bearings that are lubricated with the incorrect lubricant or with no lubricant at all resulting in excessive friction between the journal and the housing, which can excite vibrations not only in the bearing itself, but also in other parts of the rotor system. Dry whip can be also caused either by insufficient or excessive clearance [56].

## PREVENTION OF THE INSTABILITIES OCCURENCE

Upon exhibition of instabilities in the rotor system, several options are employed to reduce this behaviour. It is important to note that these corrective measures are often employed ad hoc by applying trial and error approaches [51],[50].

- *Change of lubricant viscosity and change of radial clearance* so that the combination of these parameters results in operation in the stable region. The viscosity can be changed with temperature. However, it is not possible to change the radial clearance without its construction modification.
- *Change of the bearing geometry* such that the risk of instabilities is eliminated. The most common practice is to use asymmetric geometry to create more than one pressure field, see Figure 4.3.3.

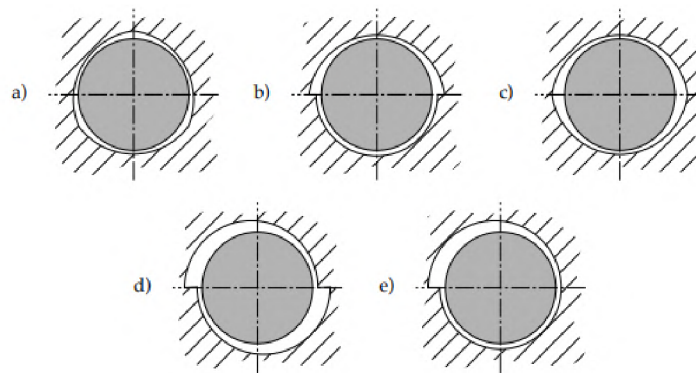


**Figure 4.3.3:** Typical geometries employed for instabilities precaution; **(a)** three-lobed; **(b)** half-lemon; **(c)** lemon; **(d)** displaced (in some literature also as offset); **(e)** spiral [59]

- *Change of the specific pressure* has stabilising effect [58], [51]. The occurrence of unstable behaviour is frequently observed in rotors that are subjected to minimal or external load. An increase in specific pressure can be achieved by increasing the radial load or by shortening the bearing. On the other hand, the stability is often sacrificed for higher frictional losses [50].

# Chapter 5

## Simulations

The current era is highly demanding in terms of speed and precision when it comes to design and manufacturing not only in the industrial sphere. The computer modelling represents one of the most valuable tools in the engineering practice. In the past, the design process was broken down into several iterative cycles, including hand calculations, drawings, cast or machined models, and load tests. This process was then repeated several times until the desired accuracy of the final product was achieved. With the help of computer technology, these repeated cycles have been mostly eliminated.

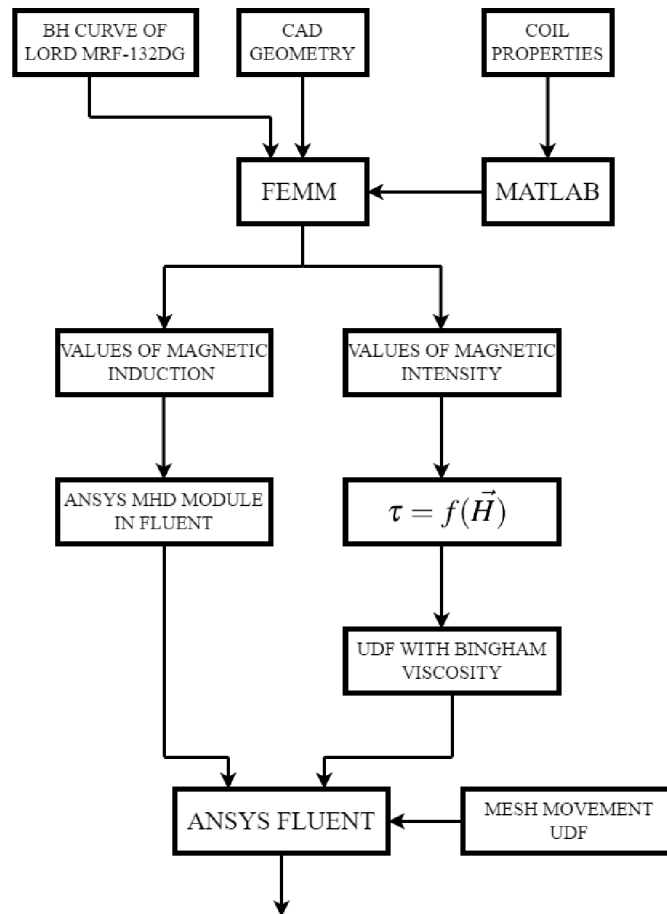


Figure 5.0.1: Schematic of the simulations process

The following sections briefly describe the theory underlying the basic virtual tools used to solve this thesis. For a correct interpretation of the results from any computational environment, it is necessary to know the theoretical foundations of the addressed scientific field. This is because the main disadvantage of virtual solvers is the possibility of physically incorrect results, due to the numerical solutions and empirical relations on which the programs are based. The core idea is a two-part simulation process consisting of magnetostatic FEMM simulation and computational fluid dynamics (CFD) simulation executed in the ANSYS Fluent software. The simulation process can be easily represented by the Figure 5.0.1.

## 5.1 FEMM Simulation

The open-source software FEMM<sup>1</sup> was selected as a suitable computational programme for magnetostatic simulation of our problem. FEMM is a suite of programmes designed to solve low-frequency electromagnetic problems in two-dimensional planar and axisymmetric domains. The programme currently addresses a range of problems, including linear/nonlinear magneto-static problems, linear/nonlinear time-harmonic magnetic problems, linear electrostatic problems, and steady-state heat flow problems [60]. One of the major advantages compared to more complex software is its speed, availability, and simplicity.

A set of Maxwell's equations is addressed, although in limiting cases. The magnetic problems addressed are those that can be considered "low frequency problems", in which displacement currents can be disregarded. Displacement currents are typically relevant to magnetic problems only at radio frequencies. The Maxwell's Equations are formulated as follows:

$$-\frac{\partial \vec{D}}{\partial t} + \text{curl} \vec{H} = \vec{j} \quad (5.1)$$

$$\text{div} \vec{D} = \rho_e \quad (5.2)$$

$$\frac{\partial \vec{B}}{\partial t} + \text{curl} \vec{E} = 0 \quad (5.3)$$

$$\text{div} \vec{B} = 0 \quad (5.4)$$

and magnetostatic problems are problems in which the fields are time-invariant. In this case, the magnetic field intensity  $\vec{H}$  and flux density  $\vec{B}$  must obey

$$\text{curl} \vec{H} = \vec{j} \quad (5.5)$$

$$\text{div} \vec{B} = 0. \quad (5.6)$$

### 5.1.1 Boundary Conditions

The boundary conditions (BC) for magnetic problems can be classified into five categories. Namely, Dirichlet BC, Neumann BC, Robin BC, Periodic BC and Antiperiodic BC [60]. In the absence of explicit boundary conditions, each boundary is assumed to be homogeneous Neumann. However, a non-derivative boundary condition must be defined somewhere (or the potential must be defined at one reference point in the domain) in order for the problem to have a unique solution.

In the case of axisymmetric magnetic problems, as in one of our cases, the condition  $\vec{A} = 0$  is enforced on the line  $r = 0$ . In this instance, a valid solution can be obtained without the need

---

<sup>1</sup>Finite Element Method Magnetics

to explicitly define any boundary conditions, provided that part of the boundary of the problem lies along  $r = 0$ .

### 5.1.2 Geometry

A sketch of the problem can be constructed on the basis of the measured dimensions of the glass tubes, the coil, and the calculated properties of the coil (Section 6.2). In order to obtain meaningful simulation results, it is necessary to consider a sufficiently large neighbourhood of the investigated body. When simulating magnetic fields, it is always necessary to bound the geometry in question by a closed curve, most often a circle. In the absence of such a curve, the formation of a computational mesh in the region outside the investigated body would not occur, rendering it impossible to evaluate the magnetic induction induced in the coil's region of occurrence outside the experimental setup. The rule of thumb for this boundary is typically at least twice the largest dimension of the setup.

It is also recommended to consider where the output parameters should be set, with the addition of auxiliary points or line segments in this area where the required quantity will be evaluated in the post-processing stage. The geometry was created using AutoCAD software, which was deemed a more convenient option than the FEMM environment. Prior to saving and importing into FEMM in DXF format, it is necessary to remove all dimensions and auxiliary structures that could compromise the integrity of the geometry. The following figure illustrates the geometry, including the boundary curve.

### 5.1.3 Case Setup and Calculation

The experiment and simulation are inspired by the paper [61]. However, the authors here perform a planar simulation, which is rather questionable from a physics point of view. The planar simulation considers the third dimension as a fictitious depth, which would imply that the coil surrounding the glass tube containing the magnetorheological fluid is in reality a set of two parallel plates, which does not correspond to reality. Consequently, we proceeded to an axisymmetric problem, which represents the problem more accurately from a physical perspective. The axisymmetry is set in the *Problem* tab.

Following the import of the geometry in DXF format, it is necessary to declare the materials in the *Properties* tab, specifically the *Materials Library*, which contains a nested database of materials with their respective properties. In our problem, there are three types of material that need to be introduced into the simulation, namely:

- Air
- Copper wiring of the coil based on the wire's diameter
- Magnetorheological liquid MRF-132DG.

In order to introduce the coil wire, it is necessary to express the wire diameter in the AWG<sup>2</sup> values, which correspond to a value of 30 AWG. As there are no magnetically active liquids within the FEMM database, the liquid in question must be inserted via *Add New Material* option. It is evident that the magnetorheological fluid exhibits nonlinear behaviour. Consequently, the

---

<sup>2</sup>American Wire Gauge System, given in ASTM Standard B 258; used since 1857 predominantly in North America. Another, less popular in recent years, is the SWG system, i.e., Standard Wire Gauge, known also as Imperial Wire Gauge or British Standard Gauge [62].



*B-H Curve* option is selected as nonlinear. Furthermore, since the behaviour of this liquid must be introduced into the software in some manner, the *Edit B-H Curve* option is selected.

The data was extracted manually from the figure 6.3.1, thus the option *Read B-H points from text file* is selected, and the B-H curve was plotted by the cubic spline derived from the entered data in the FEMM software (Figure 5.1.1). It is important to note that a recommendation in the FEMM documentation states that a minimum of three points needs to be entered, and for a good fit, we need at least ten to fifteen points.

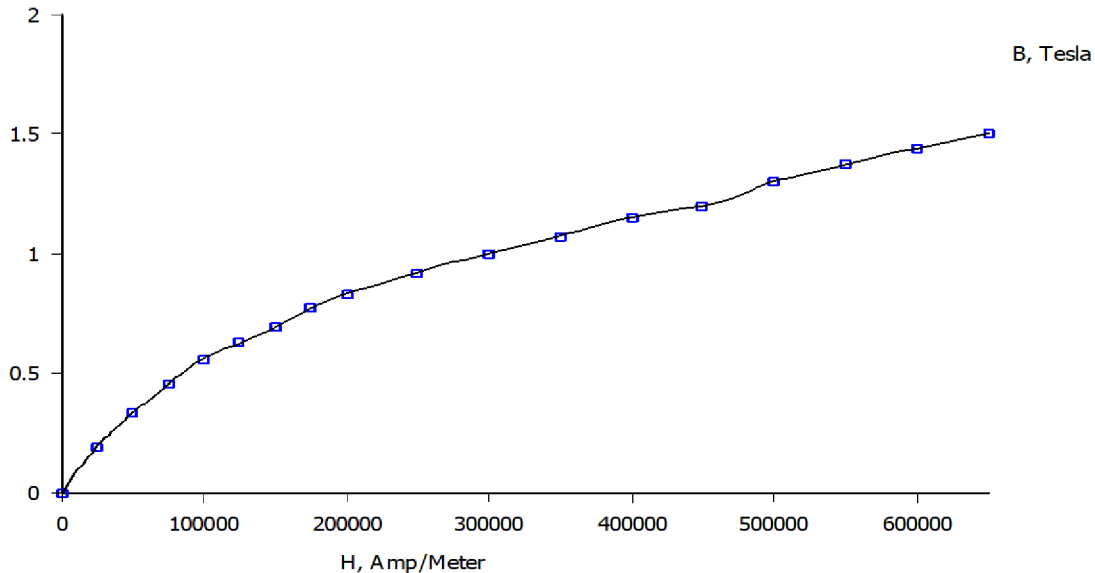


**Figure 5.1.1:** The B-H curve of MRF-132DG plotted by the FEMM software

The next step of the simulation is the definition of boundary conditions in the *Properties* tab, in the *Boundary* option. This property enables the introduction of the boundary condition  $\vec{A} = 0$  according to Section 5.1.1 with the default values set. Subsequently, the materials are allocated to their designated domains.

Since glass is not in the FEMM database of the material library, it was substituted by the *Air* material instead as both have diamagnetic properties. The properties of the coil also need to be prescribed. By selecting the options *Circuits* and *Add Property* in the *Properties* tab. We set the *Name* as coil, select the *Series* option, and set the desired current value. Lastly, the number of turns in the coil is set in the *Properties for selected block*. Now all is set for the calculation process; however, it is necessary to save the case before commencing.

### 5.1.4 Results and Post-process

The results from the simulation can be accessed with the *glasses icon* at the top bar of the user interface. For post-processing, the FEMM software provides a dedicated GUI for the visualisation of output data and the quantitative assessment of results.

Displaying the contours can be accessed at the top bar with the selection of whether we want the values of the flux or the field strength intensity. Computed values, whether the magnitude or in the normal and tangential direction, can be exported to the text file, both, for the magnetic flux density or the intensity of the magnetic field.

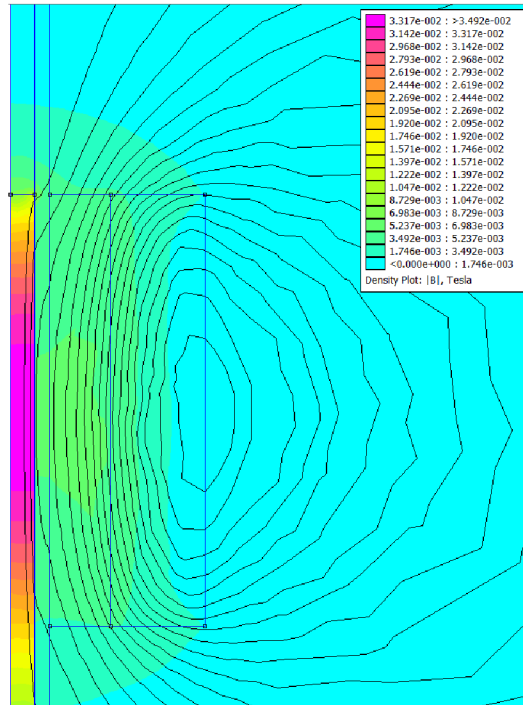


**Figure 5.1.2:** The contours of flux magnitude the case  $d_{in} = 2,4$  mm,  $I = 0,25$  A

The simulations were conducted for all three diameters of the glass tube. For the sake of interest, the problem at hand was simulated both as axisymmetric and planar. Interestingly, the glass tube with the smallest diameter, i.e.,  $d_{in} = 2,4$  mm showed higher values of magnetic flux induction magnitude than the others.

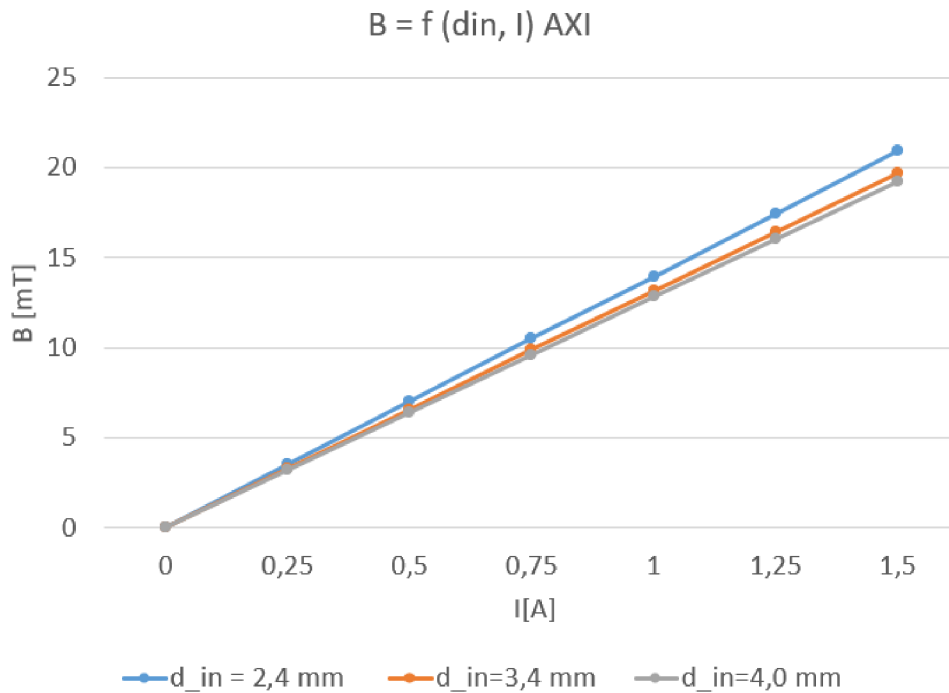


**Figure 5.1.3:** Comparison of results between the inner diameters in the axisymmetric simulation

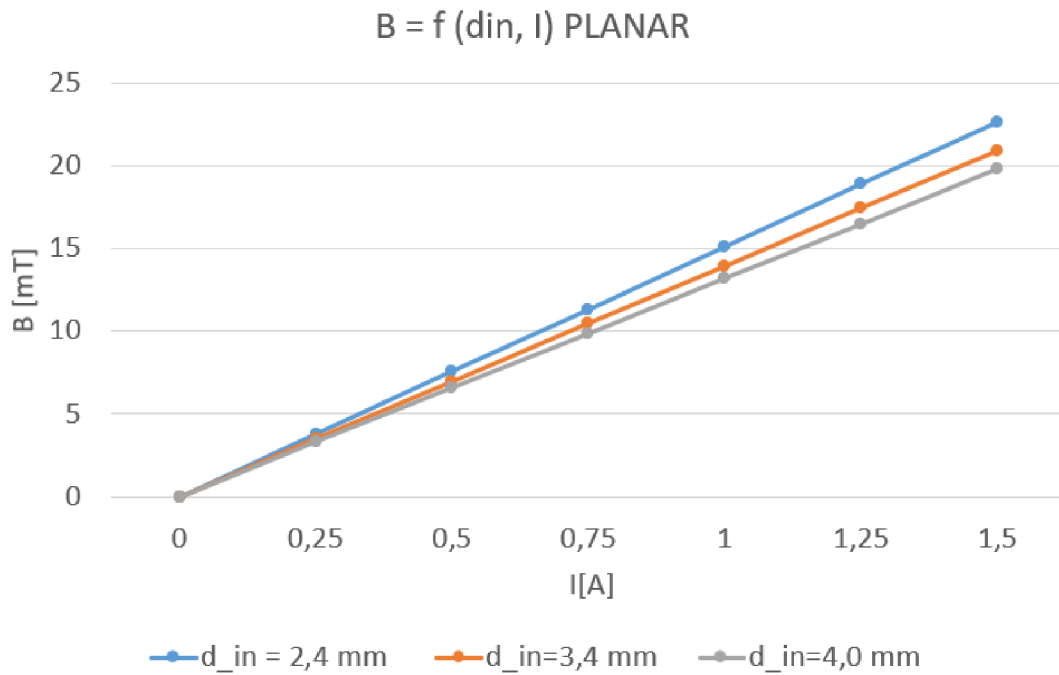


**Figure 5.1.4:** Comparison of results between the inner diameters in the planar simulation

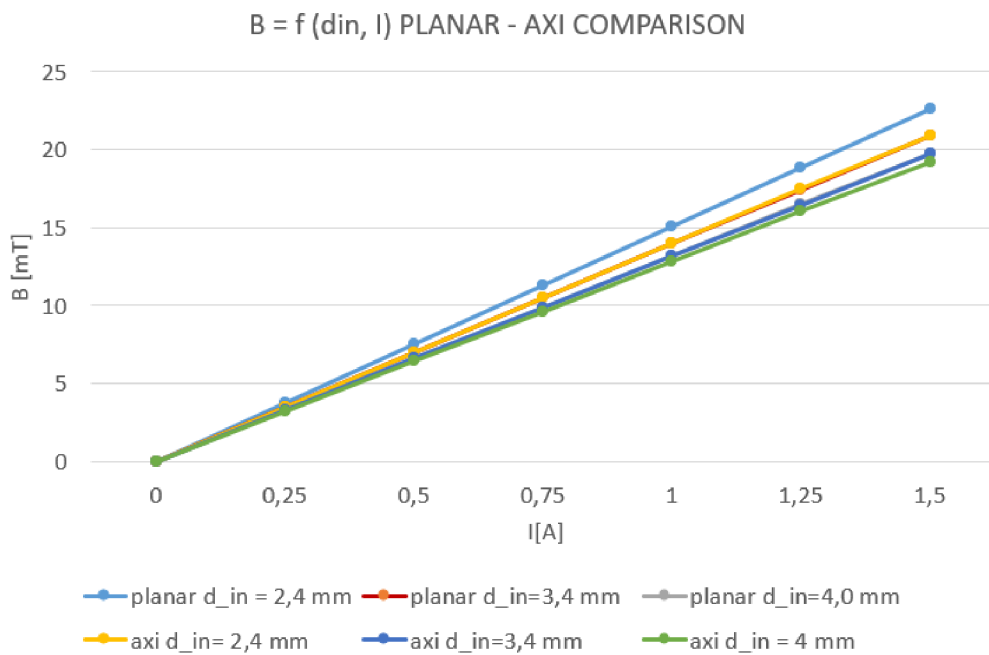


**Figure 5.1.5:** Comparison of results between the axisymmetric and planar cases

The planar simulation yields higher values, which may be attributed to the inherent characteristics of the problem. In this case, the coil is not considered a rotationally symmetric body; rather, it is treated as two parallel plates to which a third dimension is fictitiously prescribed.

## 5.2 ANSYS Fluent Simulation

The following subsections describe the procedure for the computational modelling of the 2D millifluidic channel, from geometry creation through mesh generation to the actual computational setup and its evaluation.

### 5.2.1 Geometry and Computational Mesh

The geometry of the millichannel was created directly in the ANSYS software in SpaceClaim programme and was divided into three sections for the purposes of decomposition, the establishment of named selections, and the later establishment of boundary conditions in the calculation setup.

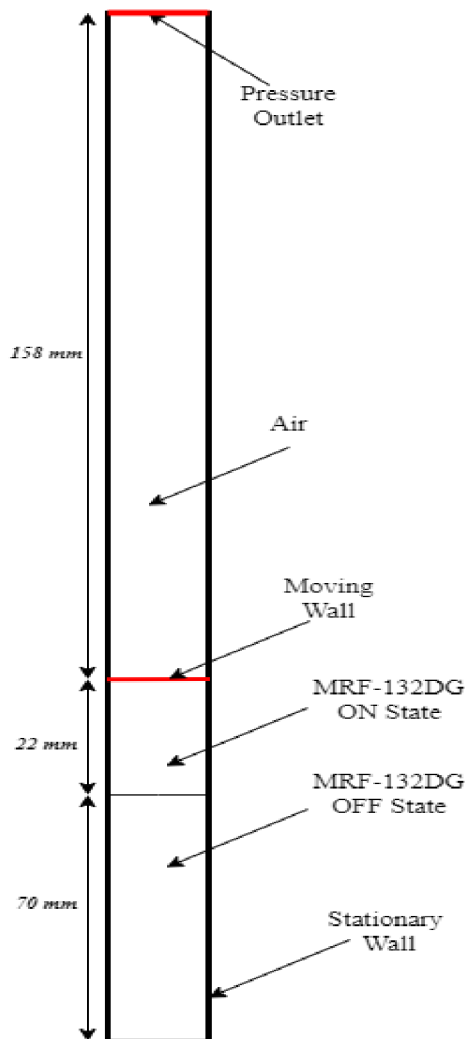


**Figure 5.2.1:** Schematic of geometry and named selections (purposefully not in scale for the sake of clarity)

In computational modelling in general, the use of structured computational meshes is the most advantageous approach in terms of the accuracy of the results and the saving of computational time. A suitable decomposition of the computational domain is a prerequisite for the use of structured meshes. The decomposition is done in such a way that only quadrilateral elements are produced in the subsequent mesh creation. The domain was imported to the ANSYS Meshing programme, and as illustrated in Figure 5.2.1, the domain in question is relatively simple in shape. The Edge Sizing function in ANSYS Meshing was employed for the creation of the mesh. This function concentrates elements primarily in the MRF-132DG ON and *Moving Wall* regions, as this is the area in which the phenomenon of interest is expected to be observed. This allowed for the rapid creation of a high-quality and structured computational mesh with low *Aspect Ratio* and zero *Skewness*. The boundary conditions for the computational domain were set, namely *Outlet* for the domain exit, *Stationary Wall* boundary condition for the perimeter walls and *Moving Wall* for the upper edge of the MRF-132DG ON region.

### 5.2.2 Calculation Configuration in ANSYS Fluent

The prepared file was transferred to ANSYS Fluent, where the calculation was performed. The model was set to *Laminar* and the gravity was turned off as gravitational forces are neglected in the field of micro- and millifluidics. As a moving mesh is also included in the simulation, it is necessary to set the time as transient.

When defining materials and their properties, three materials are considered: air, magnetorheological liquid in off and on state, i.e., MRF-132DG OFF and MRF-132DG ON, respectively. For the latter, the changeable

viscosity has to be implemented through UDF. We use the Bingham model for non-newtonian liquid by modifying the equation (2.2) as follows:

$$\tau = \tau_y + \mu \dot{\gamma} \quad / \cdot \frac{1}{\dot{\gamma}} \quad (5.7)$$

$$\frac{\tau}{\dot{\gamma}} = \frac{\tau_y}{\dot{\gamma}} + \mu \quad (5.8)$$

$$\mu_{ef(=\mu_{ON})} = \frac{\tau_y}{\dot{\gamma}} + \mu_{(=\mu_{OFF})} \quad (5.9)$$

where the ratio  $\frac{\tau}{\dot{\gamma}}$  represents the effective dynamic viscosity  $\mu_{ef}$ .

The UDF is a text file .c written in the C programming language (see Appendices) which can be employed to define, for instance, the mesh movement, speed profile on boundary conditions, and so forth an a macro is used to alter the properties of a material: DEFINE\_PROPERTY (name, c, t). The shear strain  $\dot{\gamma}$  is called from FLUENT using the command C\_STRAIN\_RATE\_MAG(c, t). In order to load the UDF successfully, it needs to be stored in the working file.

The if condition in the UDF says that if the shear strain is not equal to zero, then the value of effective viscosity is calculated according to (5.9). The else condition prevents the size of  $\mu_{ef}$  from exceeding the limits in case the value of the shear strain is zero. In this instance, a sufficiently large dynamic viscosity value of 1000 Pa.s is applied in the pre-yield region (see Figure 2.4.1), where the magnetorheological liquid behaves solid-like. The UDF is then loaded via the user-defined viscosity of the new material. The value of  $\mu_{off}$  viscosity is provided by the LORD manufacturer and the value of  $\tau_y$  depends on the intensity of the magnetic field. The values of the magnetic field's intensity were obtained from magnetostatic simulation and the value of  $\tau_y$  was then manually extracted from the manufacturer's properties as well.

The second UDF has to be introduced in order to make the mesh movement possible, see Appendices. The UDF with the mesh movement along the y-axis with frequency of 0,0025 Hz where the velocity is calculated as a function of time with an amplitude of 0,03 m/s. The UDF initialises all velocities and angular velocity components to zero and then sets only the y-component of the velocity according to the calculation.

It is now possible to set the mesh movement in the calculation's configuration, namely in the *Dynamic Mesh* with *Layering* method. We set the *Moving Wall* as a *Rigid Body* and the air and MRF-132DG ON domains as *Deforming*.

To implement the effect of the external magnetic field, a magnetohydrodynamic (MHD) module has to be enabled by command `define/models/addon-module -> 1`. Now it is crucial to follow the steps in the specific order. At fist, a "classic" hybrid initialisation has to be done, followed by an initialisation of the MHD part in its *Solution Control* tab. The *Scale Factor* can be added as well. The scale factor means that the magnetic field will be gradually increased which can have positive effects in terms of convergence of the solution. The option *Solve MHD Equation* and *Include Lorentz Force* is selected. In the MHD's *External Field B<sub>0</sub>* tab a DC field type is selected and the value of  $B_y$  is prescribed<sup>3</sup>. After these steps, we can proceed to the *Solution Methods* followed by the calculation start.

After many trials and errors, satisfying convergence of continuity was not met even at *First Order Schemes* and thus the results were incorrect from the physics perspective. An obvious fact is that this calculation requires a deeper knowledge of CFD in general, another fact is that multiphysical calculations worsen the convergence rate. Lastly, the MHD module needs further

<sup>3</sup>Again, obtained from the FEMM simulation.

in-depth analysis and further investigation of under-relaxation factors could theoretically lead to an improvement.

We can at least provide the configurations that led closest to convergence as somewhat of a stepping stone. It is worth noting, that it is generally known that the residuals of transient simulations are visually characterised by their saw-like appearance, as the residuals are restarting at every time step.

	Residuals in (-01;-02); visually correct	Residuals -03; visually incorrect
Scheme	SIMPLEC	SIMPLEC
MHD	DC $B_0$ Scale Factor: 0,001	DC $B_0$ Scale Factor: 0,001
URF <sup>4</sup>	Pressure: 0,3	Pressure: 0,2
Parameters	Number of Time Steps: 2000 Time Step Size: 4e-9 Max Iterations/Time Step: 30	Number of Time Steps: 1000 Time Step Size: 4e-9 Max Iterations/Time Step: 30

**Table 5.2.1:** An overview of different configurations of setups

# Chapter 6

## Experimental Setup Necessities

The experiment's setup and concept were influenced by [61] with a few adjustments. We have decided to observe the pressure magnitude in glass tubes with different inner diameters, namely  $d_{in} = 2,4$  mm,  $d_{in} = 3,4$  mm, and  $d_{in} = 4,0$  mm. These are the smallest diameters available from the supplier with regard to microfluidics. The experimental setup is shown in the Figure 6.4.2.

### 6.1 The Inclined-Tube Micromanometer

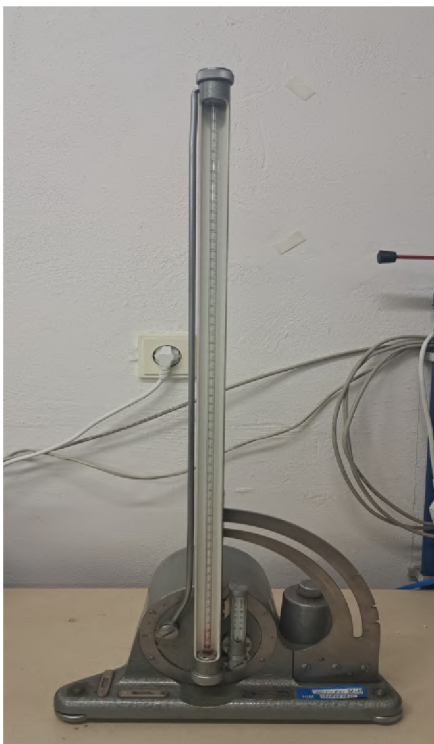


**Figure 6.1.1:** The UMK-type micromanometer with an inclined tube used in our experiment.

Due to the small pressure changes expected, accurate measurement required a suitable measurement technique. After a thorough review of the available manometers in the Viktor Kaplan Department of Fluid Engineering laboratory of heavy hydraulics, it was decided that an inclined tube micromanometer would be the best choice.

The UMK-type micromanometer manufactured by Mikrotechna-Modřany in 1969 was used for our measurements and is shown in the Figure 6.1.1. This micromanometer, whose working cartridge is usually ethanol (mercury is not recommended), allows the measurement of total pressure, static pressure, and differential pressure [63]. It is a vessel manometer whose tube can be tilted at an angle in the range ( $0^\circ; 90^\circ$ ), thus allowing the user to adjust the sensitivity of the measurement to suit their needs. By tilting the tube and reducing the angle, the range of the manometer is reduced and sensitivity is increased.

One of the advantages of this manometer is its high measurement accuracy, another is the already-mentioned possibility of changing the sensitivity and range of the manometer. However, the measurement range is relatively small, and measurements at small angles of the tube's inclination can be somewhat challenging due to the time it takes for the instrument to charge.

It is highly recommended that the cross-sections of the vessels and tubes must be constant so that the conversion rate  $e$  remains consistent. The measuring range is determined by the length of the tube. Commonly used tube lengths are 200 and 600 mm, and the accuracy is 0,01 mm. The design allows for the inclination of the arm to be adjusted in order to convert the numerical scale to 1 : 1, 1 : 2, 1 : 4, 1 : 8, 1 : 16, or 1 – 0,5 – 0,2 – 0,1 – 0,05 – 0,02. Due to its accuracy, the inclined-tube micromanometer is used for precise calibration measurements.

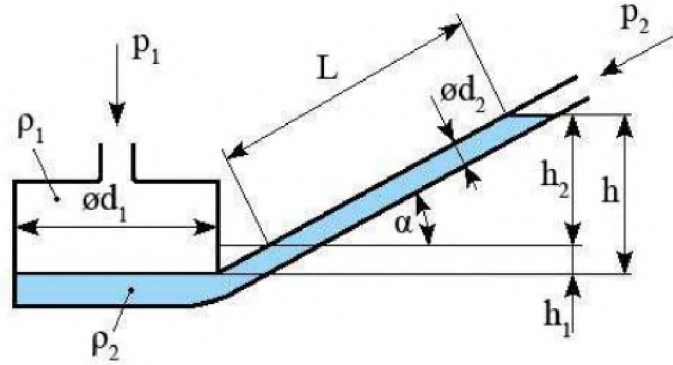


**Figure 6.1.2:** Schematic of the inclined tube micromanometer [64]

The pressure difference measured by  $\Delta p = p_1 - p_2$  is given by the formula

$$\begin{aligned} \Delta p_1 = p_1 - p_2 &= (\rho_2 - \rho_1) \cdot g \cdot (h_1 + h_2) = (\rho_2 - \rho_1) \cdot g \cdot L \cdot \left( \frac{S_2}{S_1} + \sin \alpha \right) = \\ &= (\rho_2 - \rho_1) \cdot g \cdot L \cdot e \quad (6.1) \end{aligned}$$

where  $S_1 [m^2]$  is the cross-section of the vessel,  $S_2 [m^2]$  is the cross-section of the tube, and  $L [m]$  is the deflection of the liquid column in the tube. The higher pressure is connected to the vessel and the lower pressure to the tube [64].

## 6.2 The Coil

The selection of the coil was made taking into account the operating temperature range. An increase in temperature can have a negative effect on both the performance of the coil and the stability of the magnetorheological liquid.

The solenoid valve coil was chosen from the AIGNEP catalogue [65], specifically the model SOL10012C4000 from the X1F series, which has an operating range from  $-10^\circ \text{C}$  to  $+80^\circ \text{C}$ . The dimensions of the coil can be seen in Figure 6.2.1.

However, it became apparent that the parameters provided by the manufacturer were not sufficient for our purposes. In order to proceed, it was necessary to measure some of the parameters, namely inductance  $\mathcal{L}$ , resistance  $R$  and magnetic flux  $\vec{B}$ . It was done so at the Institute of Production Machines, Systems, and Robotics at the Department of Electrical Engineering and at the Institute of Machine and Industrial Design at FME BUT. These measured values are needed to calculate the number of turns, thickness of the winding and the diameter of the wire in order to be included in the magnetostatic simulation in the open-source FEMM software.

The problem of calculating the remaining quantities is a set of algebraic equations, see Appendices where the script of the calculation is shown. Let us outline the calculation procedure.



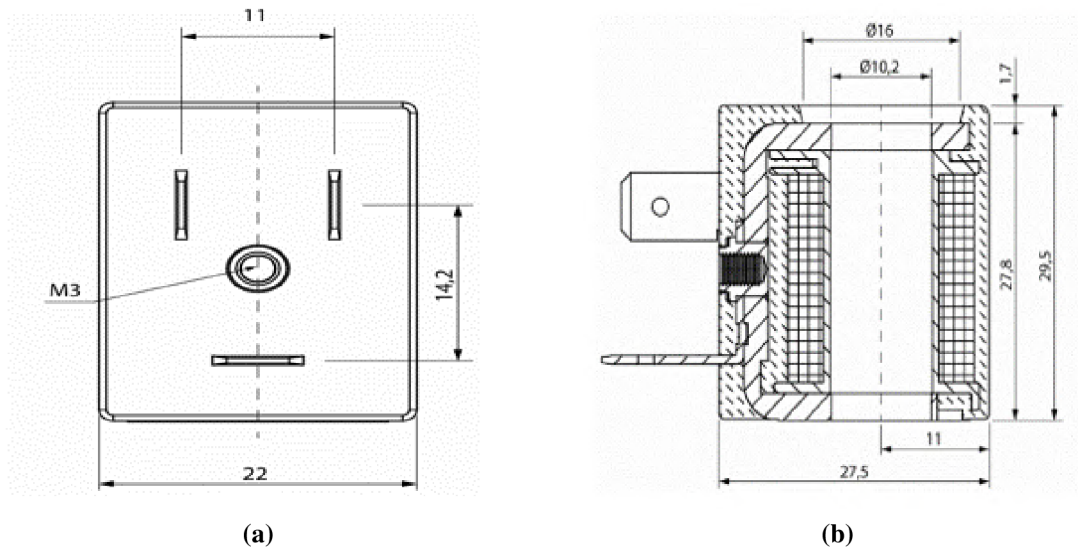


**Figure 6.2.1:** The solenoid valve coil SOL10012C4000 X1F series from AIGNEP manufacturer [65]

Firstly, it is beneficial to begin by listing the known parameters provided by the manufacturer in the following table:

$U$	$P$	$l$	$d_{in}$
[V] DC	[W]	[mm]	[mm]
12	6,5	22	10,2

**Table 6.2.1:** Parameters known from the provider

where  $U$  [V] DC is the direct current voltage,  $P$  [W] is the power,  $l$  [mm] is the length of the coil, and  $d_{in}$  [mm] is the diameter of the orifice. As already mentioned, the values for inductance  $\mathcal{L}$  [H], resistance  $R$  [ $\Omega$ ] and magnetic flux density  $\vec{B}$  were measured manually. Magnetic induction measurements have been made for various current values, see Figure 6.2.5. The material most

$\mathcal{L}$	$R$
[mH]	[ $\Omega$ ]
8,821	21,6

**Table 6.2.2:** Parameters measured manually

often used as a conductor in the coil is copper, and since we measured the coil without a core, i.e., in air, we can consider the following material constants:

$\tilde{\rho}$	$\mu_0$	$\mu_r$
[ $\Omega\text{m}$ ]	[ $\text{N/A}^2$ ] or [ $\text{H/m}$ ]	[-]
$1,69 \cdot 10^{-8}$	$4\pi \cdot 10^{-7}$	1

**Table 6.2.3:** Constants relevant for the coil calculation

where  $\tilde{\rho}$  [ $\Omega\text{m}$ ] is electrical resistivity,  $\mu_0$  [ $\text{N/A}^2$ ] or [ $\text{H/m}$ ] is called the permeability constant, and  $\mu_r$  [-] is relative permeability. To fully describe the coil and enter it into the simulation, the following quantities need to be determined:

- $N$  [-] - number of turns (winding)
- $d_{out}$  [mm] - outer diameter of the winding
- $t$  [mm] - width of the winding
- $d_w$  [mm] - diameter of the wire

To do so, the following formulas are used:

$$N = \frac{Bl}{\mu_0 \mu_r I}. \quad (6.2)$$

Since the number of turns  $N$  must be an integer, it was rounded to 94. The diameter of the wire is calculated as:

$$d_w = \frac{l}{N}, \quad (6.3)$$

the width of the winding:

$$t = \frac{2 \cdot N \cdot d_w}{l}, \quad (6.4)$$

and finally, the outer diameter:

$$d_{out} = d_{in} + 2t. \quad (6.5)$$

$N$	$d_w$	$t$	$d_{out}$
[-]	[mm]	[mm]	[mm]
93,37	0,24	2,00	4,01

**Table 6.2.4:** Calculated quantities

Since the number of turns  $N$  must be an integer, it was rounded to 94. The results were consulted at the Institute of Production Machines, Systems, and Robotics at the Department of Electrical Engineering at FME BUT. Upon initial observation, it appeared that this coil would be sufficient for our intended purposes, with the radial gap between the coil and the glass tube containing the magnetorheological fluid being of negligible consequence. Subsequent to this, initial magnetostatic simulations were conducted.

However, these yielded results that were in stark contrast to the measurements, prompting the need for a second round of measurements, this time conducted at Institute of Machine and Industrial Design at FME BUT, where, as was subsequently found, they have extensive experience with these fluids. The Figure 6.2.2 shows the setup of the coil measurement.

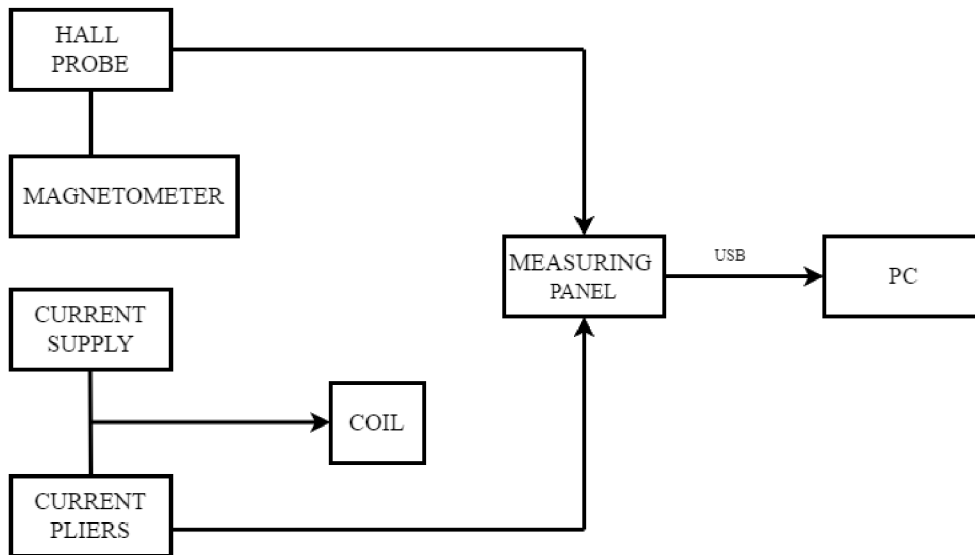


**Figure 6.2.2:** Coil measurement scheme

The coil was measured with magnetometer F. W. BELL 180 GAUSS/TESLAMETER with accuracy is  $\pm 1\%$  deflection. The principal drawback to the utilisation of the Hall probe in magnetometers is that they are highly susceptible to disturbances in the form of displacements and deflections. It is therefore of the utmost importance to identify the specific points where measurements will be taken prior to the commencement and it is also crucial to recognise that the Hall probe will only yield valid results if it is positioned perpendicular to the magnetic field lines.

In order to facilitate the measurements, a point was selected that lies on the imaginary axis of rotational symmetry at a height of approximately 2,5 mm, as illustrated in the Figure 6.2.3.



**Figure 6.2.3:** Coil measurement with Hall probe

The measurements were done for values of the input current 0,25, 0,5 up to 1,5 A. At the value of 1,5 A the coil would start to generate heat and therefore the measurement was aborted for the sake of safety. The obtained data, both from the measurement and the calculation, were then put to the magnetostatic FEMM simulation. Another reason why the FEMM simulation of the coil solely was carried out is due to the fact that in order to quantify the desired observation, the magnetic field needs to be estimated because it is not possible to place the Hall probe in the glass tube arrangement.

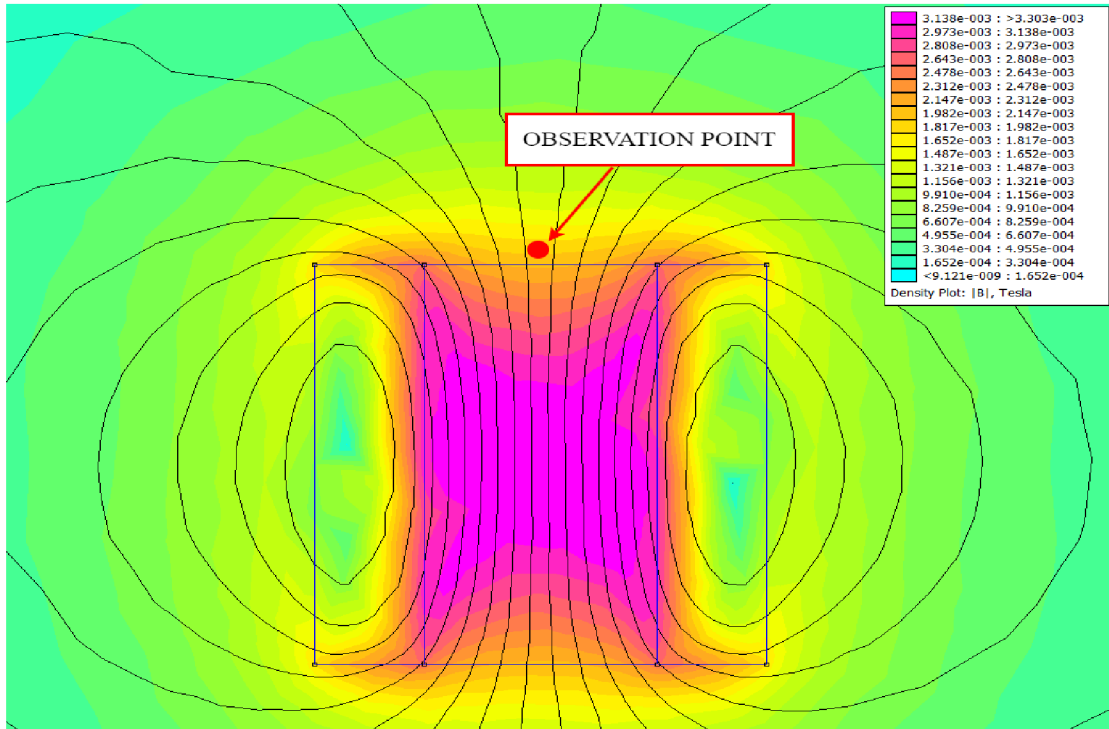


**Figure 6.2.4:** FEMM simulation result for the case  $I = 1A$

On the description and the setup of the magnetostatic simulation see Section 5.1. A comparison between the measurement and the simulation carried out can be seen in the Figure 6.2.5.

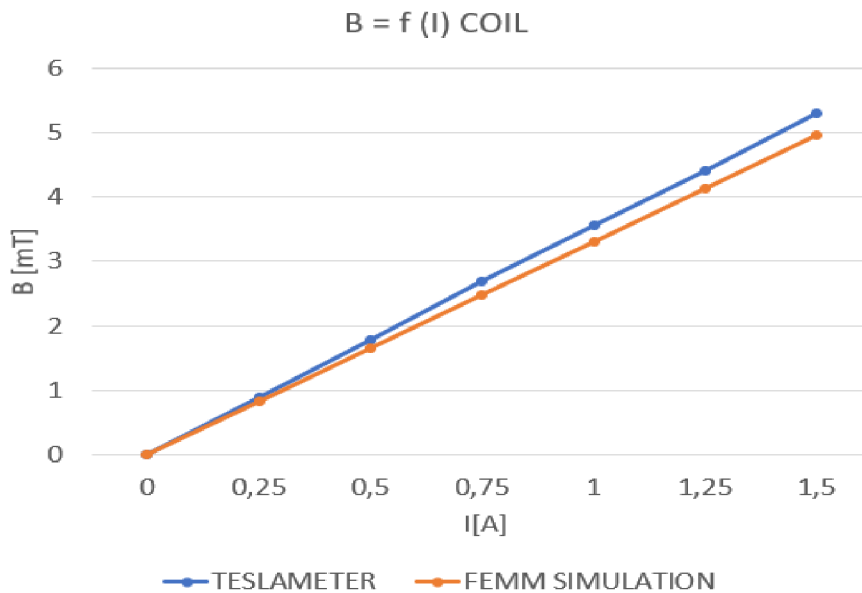
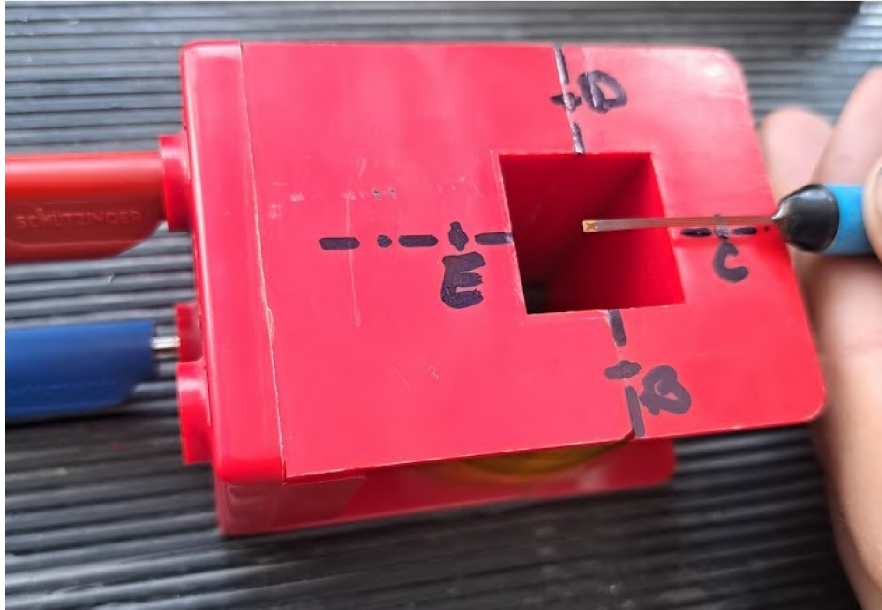
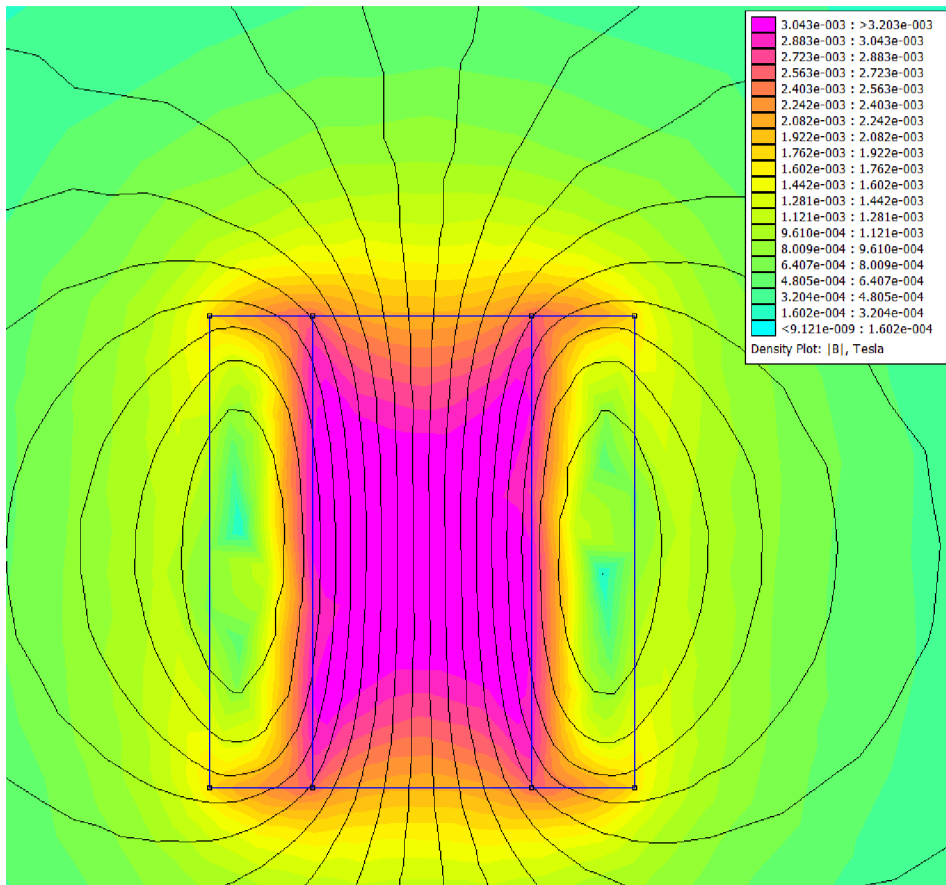


**Figure 6.2.5:** Comparison results between the teslameter measurement and simulation

Another coil that was at our disposal was measured whether it could generate stronger magnetic field. It turned out that the magnetic induction was even lower at the observation point since the coil started to overheat at only 0,06 A.



(a)



(b)

**Figure 6.2.6:** Measurement of the second coil with properties  $N=100$ ,  $d_w=2\text{mm}$  (AWG 12),  $d_{in}=2\text{ cm}$  at  $I=0,06\text{ A}$ ,  $B=3,14\text{ mT}$

## 6.3 LORD MRF-132DG

In our experiment, we used the hydrocarbon-based magnetorheological liquid LORD MRF-132DG from the LORD Corporation. Here are its properties, which can be found on the manufacturer's website [66].

- *Appearance:* Dark gray liquid
- *Viscosity:*  $0,092 \text{ Pa} \cdot \text{s}$
- *Density:*  $2,95 - 3,15 \text{ g} \cdot \text{cm}^{-3}$
- *Solids content by weight:* 80,98 %
- *Flash point:*  $> 150^\circ$
- *Operating temperature:*  $-40^\circ \text{ C}$  to  $+130^\circ \text{ C}$

Additionally, the manufacturer provides a diagram illustrating the relationship between magnetic induction  $B$  and magnetic field strength  $H$  (6.3.1) along with a diagram illustrating the relationship between yield stress  $\tau_y$  and magnetic field strength  $H$  (??).

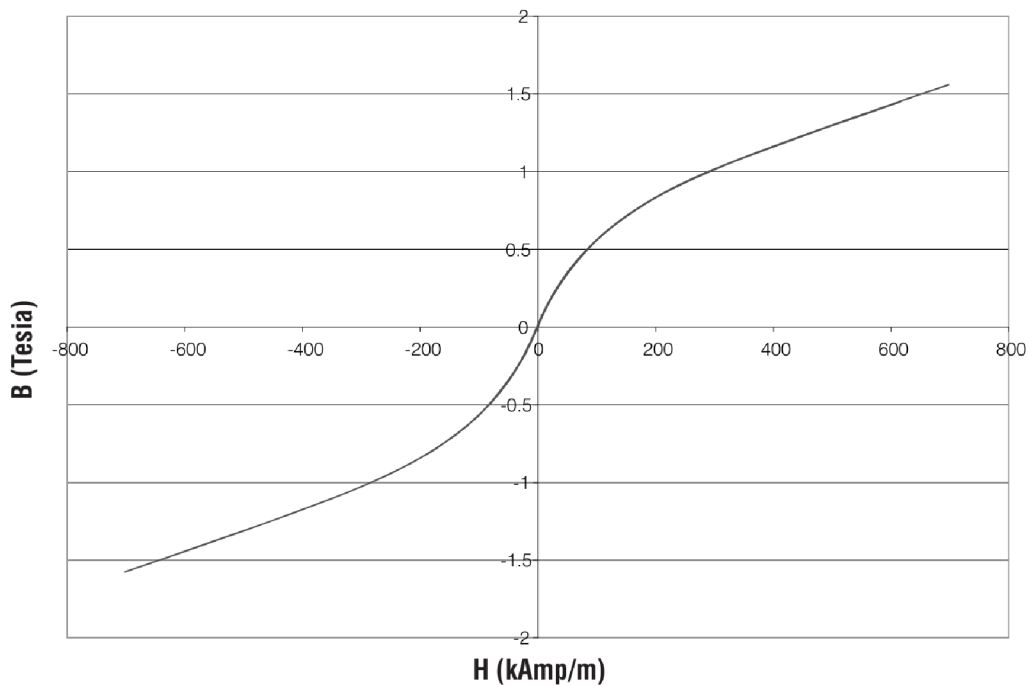


**Figure 6.3.1:** B-H curve of the magnetorheological liquid MRF-132DG [66]

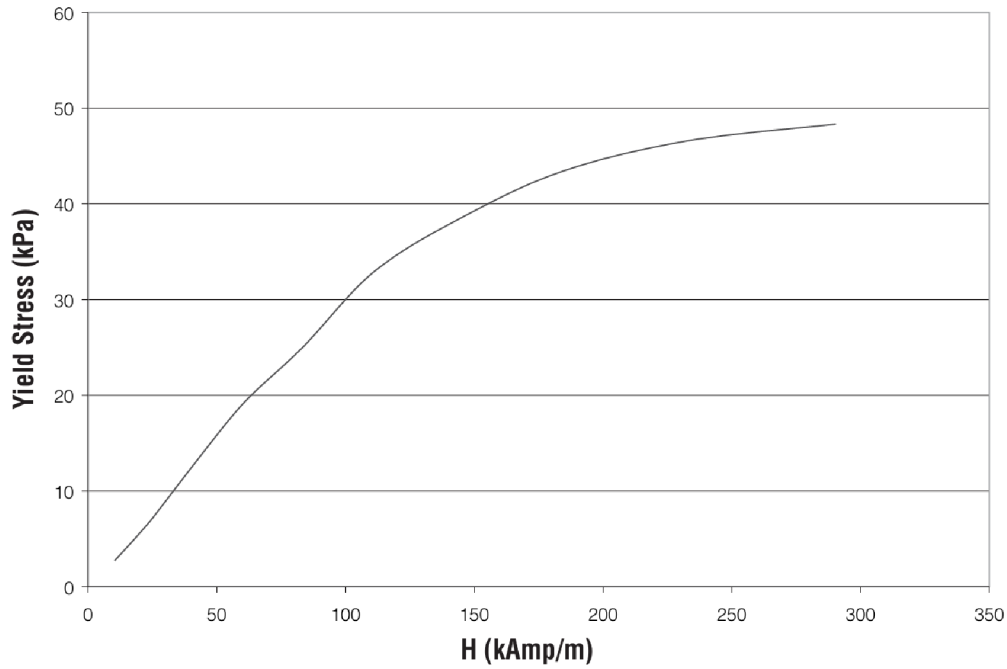


**Figure 6.3.2:** The relationship between yield stress  $\tau_y$  and magnetic field strength  $\vec{H}$  of the magnetorheological liquid MRF-132DG [66]

One of the disadvantages of magnetorheological liquids in general is their sedimentation tendency. This is something that we encountered in our department. Nevertheless, from the information provided by the Institute of Machine and Industrial Design at FME BUT, we know that the liquid is chemically stable. Furthermore, as the manufacturer states, it is possible to use a paint shaker to homogeneously redisperse the particles again, if necessary. With this in mind and with the help of an improvised device with a propeller, the liquid was left to mix for several hours.

No separation was observed between the particles and the carrier fluid under common manipulation. A separation occurs in static conditions if left untouched for a longer period of time, i.e., days, but low-shearing agitation (shaking or remixing) prior to use would easily redisperse the particles into the previous state.

# 6.4 The Method

In this section, we will compare our configuration with that of the authors Widodo and Ubaidillah from [61], [67] and [68]. The distinction, which is apparent at a first glance from the Figure 6.4.1, is the configuration methodology selected by the authors.

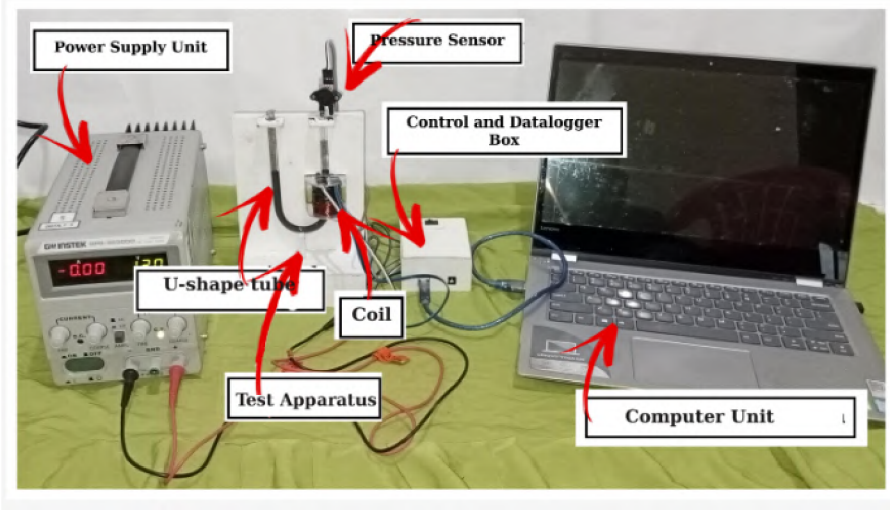


Figure 6.4.1: The configuration by authors [61], [67] and [68]

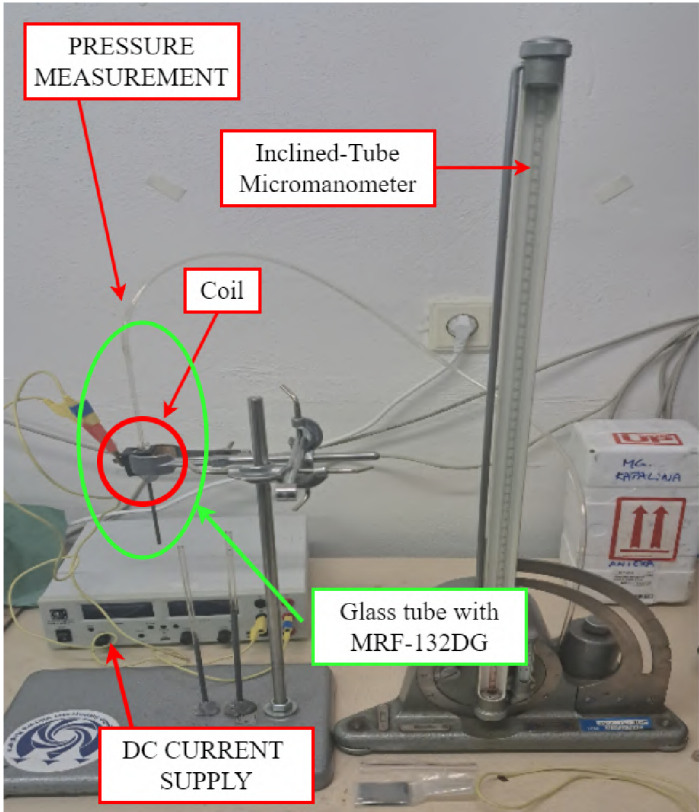


Figure 6.4.2: The configuration by us

The main differences are in the way the pressure is sensed, the cycling of the delivered current is controlled and the way the data is recorded. For the reasons mentioned above, our



configuration is manual rather than digital. Another difference is in the chosen vessel, where authors opted for the U-shaped glass tube with inner diameter  $d_{in} = 5$  mm, whereas we chose glass tubes with inner diameters  $d_{in}=2, 4$  mm,  $3, 4$ mm and  $4$  mm as we were also interested on the relation between the magnetic flux induction generated in dependence on the volume of the magnetorheological liquid contained within.

Lastly, the difference is in the electromagnetic coil. It seems that the authors had their coil customised so it would fit on the glass tube with minimal to none radial clearance. The same coil test with Teslameter and the verification in FEMM software was conducted by both parties, Figure 6.2.3, 6.3.2.

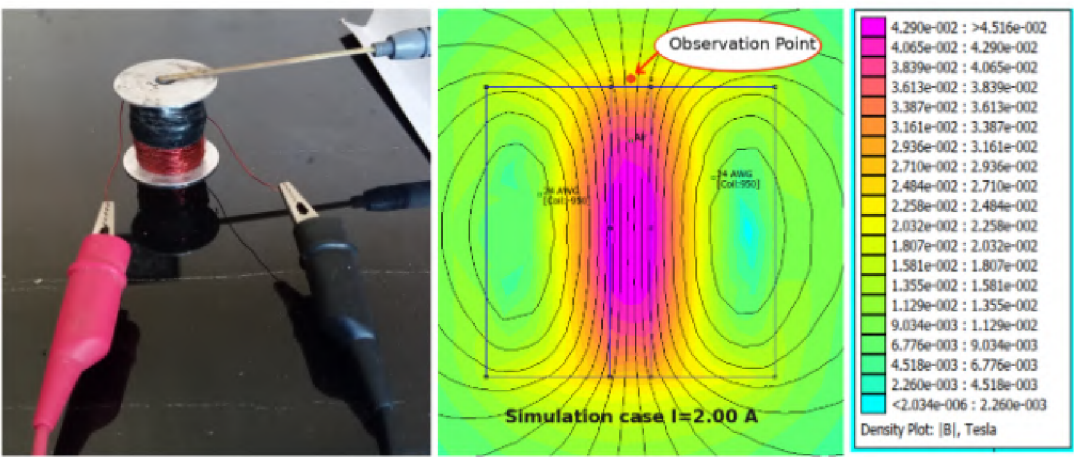


**Figure 6.4.3:** The test with Teslameter and test simulation in FEMM software by [61], [67] and [68]

The data validation of both parties shows similar trend

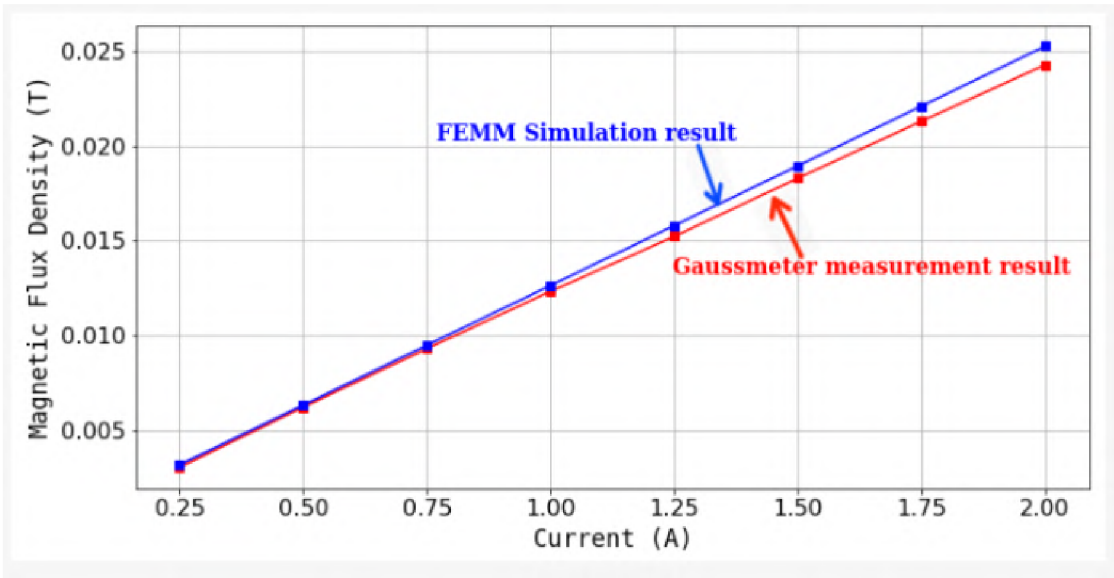


**Figure 6.4.4:** The validation of the measured values and coil simulation [61], [67] and [68]

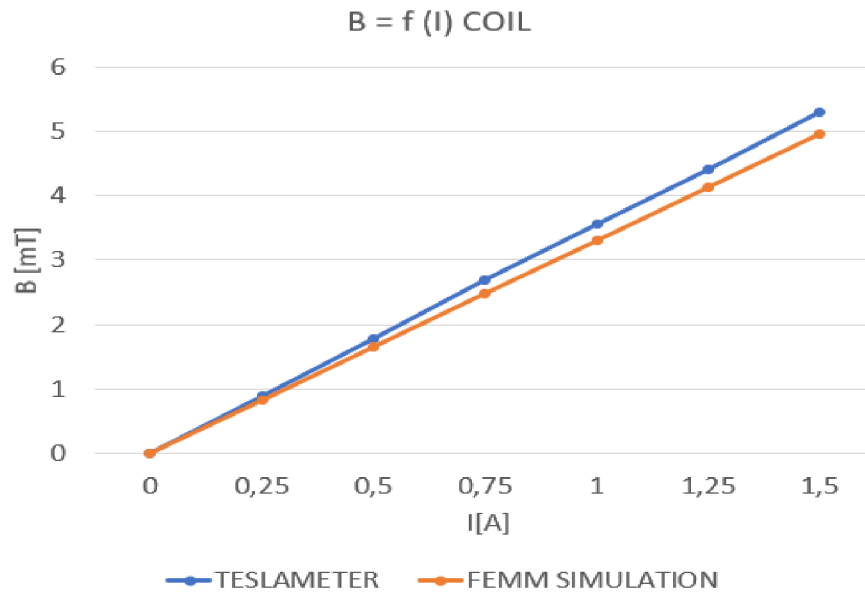


**Figure 6.4.5:** The validation of the measured values and coil simulation by us

The authors also used an Arduino microcontroller unit and graphical serial device terminal that served as a data logger. Prior to the supply of the DC current a magnetorheological liquid would be poured into the U-tube. The authors used MRF-122DG, whereas our liquid is MRF-132DG, both having similar properties. The pressure changes are monitored using the pressure sensor and recorded using the data logger at sampling speed 10 ms. The results obtained by magnetostatic simulation of the FEMM would be performed at each level of increased current, as in our case. The only difference is that due to their setup, only planar case could be evaluated.

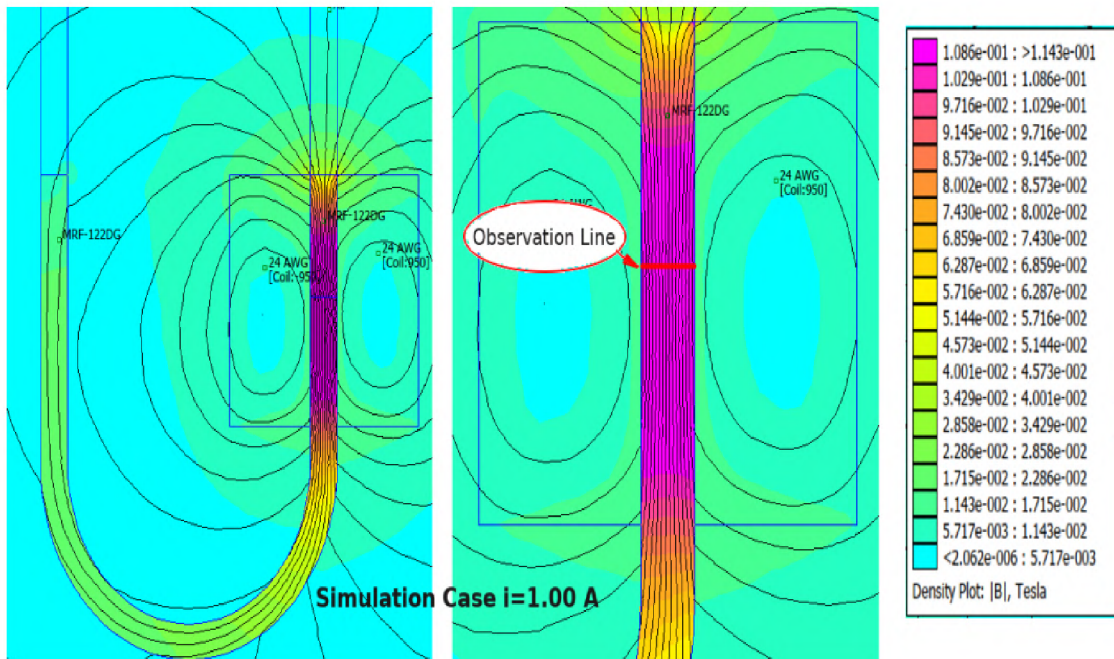


**Figure 6.4.6:** Results of the FEMM simulation for the case  $I = 1$  A by [61], [67], and [68]

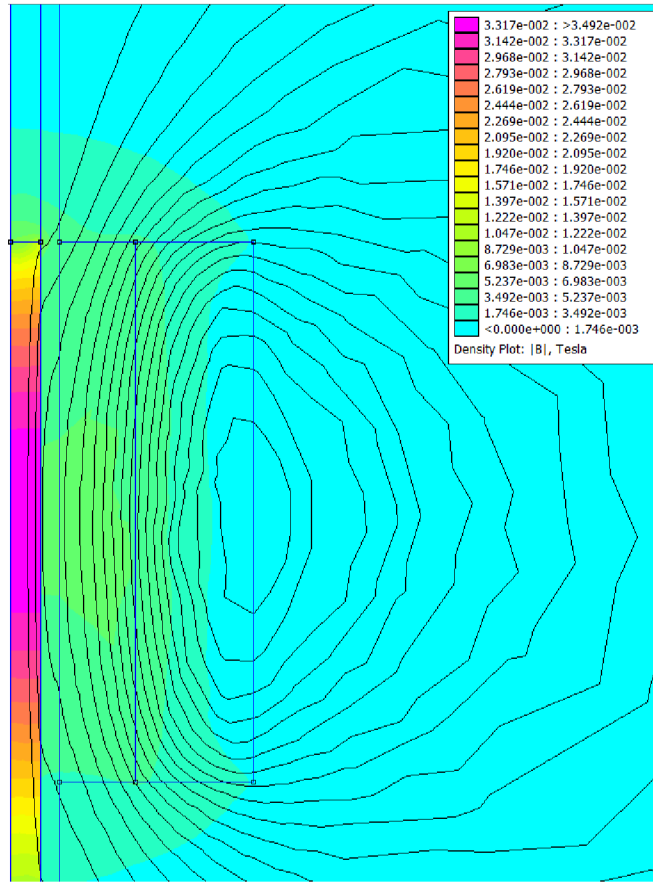


**Figure 6.4.7:** Our results of the FEMM simulation for  $d_{in} = 2,4$  mm,  $I = 0,25$  A

A correlation of the same trend was observed in both parties, however due to our coil being greatly weaker, the values of magnetic induction generated were lower as well.

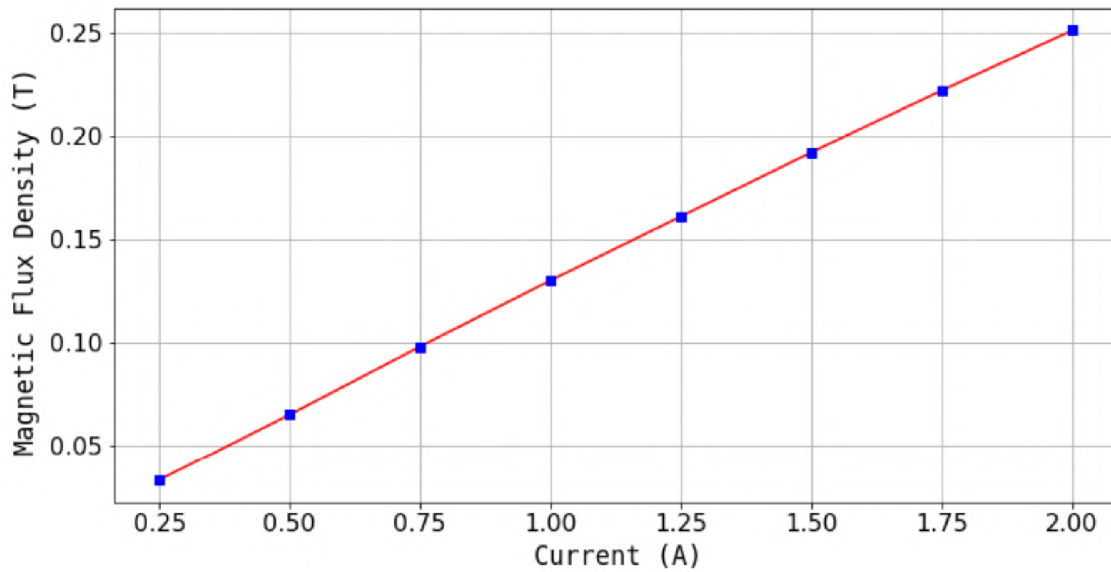


**Figure 6.4.8:** The correlation between magnetic induction and current from FEMM simulation by [61], [67] and [68]

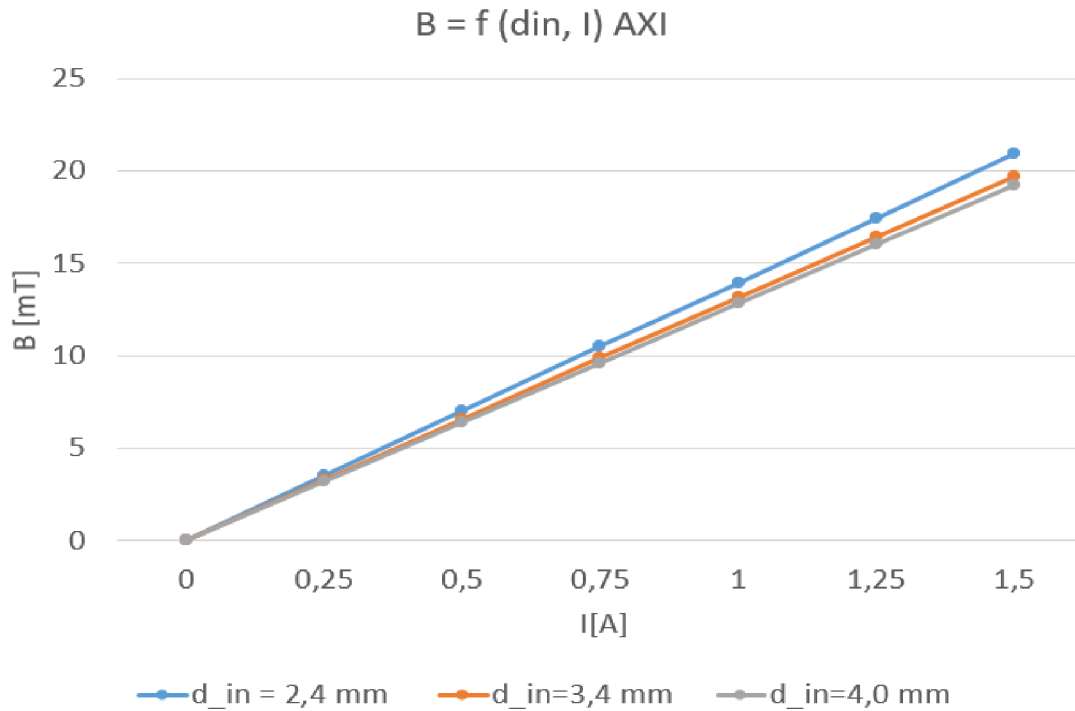


**Figure 6.4.9:** The correlation between magnetic induction and current from FEMM simulation by us

Despite our best attempts of trying to generate pressure difference, no pressure was generated mainly due to the poor choice of the coil. Let us present the pressure generated by the authors [61], [67] and [68].

Current Input (A)	0.25	0.50	0.75	1.00	1.25	1.50	1.75	2.00
$\Delta P_{min}$ (Pa)	13.06	58.98	129.17	244.49	496.04	679.79	867.36	835.50
$\Delta P_{max}$ (Pa)	18.39	65.91	155.64	292.53	533.77	739.02	942.50	120.01
$\Delta P_{avg}$ (Pa)	15.53	62.80	144.77	267.80	517.16	709.20	904.64	918.55
$\Delta P_{median}$ (Pa)	15.34	63.16	147.14	267.09	519.42	708.99	904.34	909.34
Std Deviation	2.68	3.12	11.52	21.29	15.63	25.85	38.37	78.84

**Table 6.4.1:** where  $\Delta P_{min}$  is the minimum pressure change that occurs during magnetisation at the observation cycle at each given current,  $\Delta P_{max}$  is the maximum pressure change that occurs during magnetisation at the observation cycle at each given current,  $\Delta P_{avg}$  is the average pressure change that occurs during magnetisation at the observation cycle, Std Deviation is the standard deviation of the measured pressure.

While setting up the experiment a question was raised regarding the potential impact of the radial air gap of few millimetres between the coil and the glass tube affecting the experiment negatively. The initial estimate, discussed at the Institute of Production Machines, Systems, and Robotics at the Department of Electrical Engineering, was that the effect would be negligible. However, later when the measurement of the coil was conducted at the Institute of Machine and Industrial Design, it was revealed to us that, not only it will have severe consequences, but also the chosen coil would be proven to be too weak to generate any significant pressure increase.

# Chapter 7

## Discussion

### 7.1 The Experiment

In a Poiseuille flow channel configuration, it is known that the magnetic field generates a pressure difference and regulates a pressure drop, as occurs in the valve mode of operation [69]. In a Poiseuille flow arrangement, the pressure difference is generated by the obstruction of the existing fluid flow. Consequently, the measured pressure difference is identified as the flow pressure drop that occurs due to obstruction.

The experiment in this thesis is designed to investigate the potential for the magnetic field to exert pressure on the magnetorheological liquid while at rest. The experiment would be conducted using a glass tube. Initially, the tube would be set at rest, and then the magnetic field would be applied by gradually increasing the current input to the coil via the source.

It is anticipated that a visual change in the liquid level would be evident. This change would be caused by the magnetic induction of the magnetic particles immersed in the magnetorheological liquid, which provides magnetic force attraction to the particles until they reach equilibrium.

In order to validate the observation, it is necessary to estimate the magnetic field, as it is not possible to insert the Teslameter probe into the glass tube. Therefore, a FEMM simulation was carried out to simulate the magnetic field that would exist in the theoretical model of our arrangement.

The control input variable is the direct current (DC) supply with a voltage of 12 V and variable currents, which are used to generate varying magnetic field strengths in the magnetorheological liquid. The current variations are 0, 25 A, 0,5 A and so on until a limit is reached.

It is known that the efficiency of magnetically active liquids tends to degrade with rising temperature, as well as that of the coil. Therefore, the measurement would continue until such a limit is reached. In the case of [61], a different configuration was used with a different fluid, and the limit was reached at 2 A. Therefore, a similar estimate is expected.

Prior to the application of a direct current (DC) current, a magnetorheological liquid MRF-132DG was poured into glass tubes using a syringe. Every 10 seconds, the current would alternate between zero and a given value. The changes in pressure would be monitored with an inclined-tube micromanometer and recorded manually. A linear correlation between magnetic induction  $\vec{B}$  and the current  $I$  is expected.

It is anticipated that a gradual increase in pressure will be accompanied by a corresponding rise in the liquid level, with a similar trend observed across the input currents. The magnetic simulations (see Figure 6.4.7) indicated the presence of a magnetic field around the electromagnetic coil and the field line coinciding with the liquid in a parallel direction. Consequently, it is

expected that micrometre-sized particles will form a chain-like structure along the field lines, which differs from the conventional induction-liquid arrangement observed in the valve mode.

The switching between the OFF and ON states is expected to result in the magnetic particles dispersed in the liquid retaining their chain-like structure due to their magnetic remanence, where a magnetic hysteresis would play a key role as a few second window at the OFF state would not be enough for the particles to redisperse to their initial state. Consequently, each new switch to the ON state would benefit from the previous step as the initial point would be higher for each new cycle. Thus, a slightly increasing pressure slope would be noticeable. It is anticipated that the values would be within the range of a few Pascals, with the highest value being in the hundreds of Pascals at most.

*Note:* While setting up the experiment a question was raised regarding the potential impact of the radial air gap of few millimetres between the coil and the glass tube affecting the experiment negatively. The initial estimate, discussed at the Institute of Production Machines, Systems, and Robotics at the Department of Electrical Engineering, was that the effect would be negligible. However, later when the measurement of the coil was conducted at the Institute of Machine and Industrial Design, it was revealed to us that, not only it will have severe consequences, but also the chosen coil would be proven to be too weak to generate any significant pressure increase.

Therefore, new objectives, regarding the design improvement, were set and are yet to be implemented. These include a 3D print of the coil's base bobbin for each case of the glass tubes, such that there is no radial gap. Then, next iteration of magnetostatic simulation would be carried out and customised wiring would be done.

## 7.2 Usage Proposal - A Concept Idea

As already mentioned in one of previous chapters, the principle of symmetry is often used in engineering practice, and the following configurations of hydrodynamic journal bearings and channels containing magnetorheological fluid are intuitively proposed:

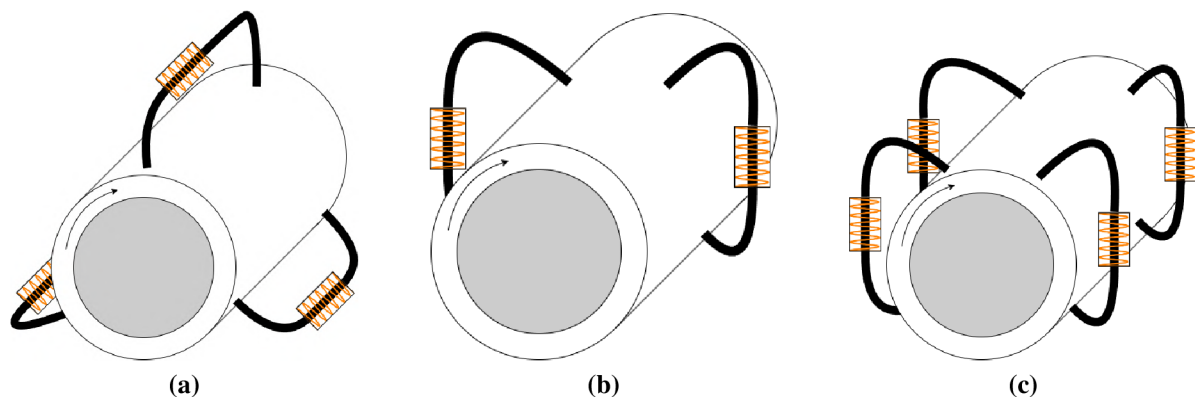


**Figure 7.2.1:** Suggested concepts of journal bearing with magnetorheological liquid in micro- or millichannels, from left to right: (a) Channels in the axial direction with a circumferential angle of  $120^\circ$ ; (b) Channels in the radial direction; (c) Multiple channels in the radial direction.

In conjunction with these proposals, a number of questions arise:

- What material should be selected for the channels themselves?
- How should the installation of the channels be carried out?
- Will the installation of the channels compromise the integrity of the bearing itself?
- How should the bearing mounting be solved for a particular modification?
- How can the magnetorheological fluid be ensured not to leak out of the channels in an unactivated state and damage the journal or bearing pan by abrasion by ferromagnetic particles?
- Whether the control process could be automated, for example, by a programmable logic controller (PLC)?

Further research, in collaboration with other departments, is necessary to answer these questions. In order to do so, structural design, strength design, and finite element method calculations would be required. Additionally, studies, including calculations, would need to be carried out on the interaction of the magnetic liquid with the structure. Finally, a process for automation would need to be developed as well.

In the context of simulations, it would be reasonable to consider conducting a magnetic simulation, for instance, in ANSYS Maxwell software, and subsequently coupling it with ANSYS Fluent software, as this could lead to promising results.

# Conclusion

Within the framework of this thesis, thorough research on a multidisciplinary topic was carried out. In this research, the topics of magnetism, magnetically active liquids, fluid mechanics fields at micro- or millirange, and the issue of lubrication-induced instabilities in journal bearings were introduced.

A comprehensive examination of the subject matter, coupled with an analysis of devices such as seals, clutches, dampers, and numerous others, led to the identification of a field of study that would facilitate the determination of which component would be the focus of attention. The sphere of journal bearings and their lubrication-induced instabilities was selected as an appropriate field of study to conceptualise a method for optimising or potentially reducing the undesirable phenomenon.

An investigation was conducted, which led to the design and construction of an experiment. Despite the promising concept, a factor that initially appeared to be of little consequence had a detrimental impact on the practical implementation of the experiment, rendering it unfeasible. Nevertheless, the thesis offers recommendations for the next iteration of the procedure, which will ultimately lead to the final measurement.

The computational simulations are divided into two levels. The first level employs the finite element method for electromagnetism problems in FEMM software. The second level utilises the finite volume method in ANSYS Fluent software for CFD calculations. The input parameters for the magnetostatic simulation are the so-called  $B - H$  curve of the used magnetorheological fluid MRF-132DG from the manufacturer, the dimensions of the designed experiment, and the properties of the used coil. The outputs of this simulation are values of magnetic induction and magnetic field strength. These values will serve as input in the second level of simulation, i.e., CFD. The magnetohydrodynamic module is employed, which extends beyond typical user capabilities. Here, the influence of the external magnetic field is incorporated. The magnetic field strength values are employed to obtain the yield stress values of the magnetorheological fluid; the graphical expression is provided by the manufacturer. The yield stress values are then implemented in the so-called user-defined function in the Bingham model of the non-Newtonian fluid. Furthermore, the moving computational mesh is also implemented using the user-defined function, given that translational motion in the direction of excitation from the coil is to be expected.

Although the practical outcome was not as successful as hoped, the knowledge gained can be built upon in future iterations of research and provide a solid foundation for possible future applications in this direction, which could lead to significant innovations in various engineering and scientific fields. A reasonable approach would be customised design and winding of the coils such that there is no radial gap as the use of commercially available coils is rather insufficient and the specific needed configuration, i.e. the orifice and wiring, is unobtainable.

When it comes to the CFD simulation, the MHD module needs further in-depth analysis and further investigation of under-relaxation factors could theoretically lead to an improvement of



convergence rate. Another way that could lead to promising outcome is either coupling the Ansys Maxwell with Ansys Fluent software, or using completely different computational software such as OpenFoam.

# References

1. WALKER, Jearl; HALLIDAY, David; RESNICK, Robert. *Fundamentals of Physics: Extended*. 10th ed. Hoboken: Wiley, 2014. ISBN 978-1-118-23072-5.
2. SEDLÁK, Bedřich; ŠTOLL, Ivan. *Elektřina a magnetismus*. 3rd ed. Praha: Karolinum, 2012. ISBN 978-80-246-2198-2.
3. KŘIŽÁKOVÁ, V. *Magnetické vlastnosti materiálů založených na metastabilních vrstvách Fe-Ni*. Brno, 2016. Bakalářská práce. Vysoké učení technické v Brně, Fakulta strojního inženýrství. Supervised by Ing. FLAJŠMAN Lukáš.
4. SVOBODA, Emanuel. *Přehled středoškolské fyziky*. 4., upr. vyd. Praha: Prometheus, 2005. ISBN 978-80-7196-307-3.
5. BIN MAZLAN, Saiful Amri. *The Behaviour of Magnetorheological Fluids in Squeeze Mode*. Dublin, 2008. PhD thesis. Dublin City University.
6. FIALOVÁ, Simona; POCHYLÝ, František. A New Formulation of Maxwell's Equations. *Symmetry* [online]. 2021, vol. 13, no. 5, p. 868 [visited on 2022-11-02]. ISSN 2073-8994. Available from DOI: 10.3390/sym13050868.
7. *Comparison of B, H and M inside and outside a cylindrical bar magnet* [Online]. San Francisco, CA: Wikimedia Foundation, 2024. [https://en.wikipedia.org/wiki/Magnetic\\_field#/media/File:VFpt\\_magnets\\_BHM.svg](https://en.wikipedia.org/wiki/Magnetic_field#/media/File:VFpt_magnets_BHM.svg). [cit. 2024-05-08].
8. SAMYA. *Magnetic field lines in physics* [Online]. 2024. [https://stock.adobe.com/cz/images/magnetic-field-lines-in-physics/527899867?asset\\_id=527899867](https://stock.adobe.com/cz/images/magnetic-field-lines-in-physics/527899867?asset_id=527899867). [cit. 2024-05-08].
9. ODENBACH, S. Ferrofluids — Magnetically Controlled Suspensions. *Colloids and Surfaces A: Physicochemical and Engineering Aspects*. 2003, vol. 217, no. 1–3, pp. 171–178. Symposium C of the E-MRS 2002 Spring Meeting in Strasbourg, France.
10. ODENBACH, S.; THURM, Steffen. Magnetoviscous Effects in Ferrofluids. In: 2008, pp. 185–201. ISBN 978-3-540-43978-3. Available from DOI: 10.1007/3-540-45646-5\_10.
11. PŘIKRYL, M. *Hydrodynamické tlumiče na principu magnetické kapaliny*. Brno, 2017. Diplomová práce. Vysoké učení technické v Brně, Fakulta strojního inženýrství. Supervised by prof. Ing. CSc. POCHYLÝ František.
12. GENC, S.; DERIN, B. Field Responsive Fluids - a Review. *Key Engineering Materials*. 2012, vol. 521, pp. 87–99. <http://www.scientific.net/KEM.521.87>. Dostupné z: <http://www.scientific.net/KEM.521.87> [Citováno: 10. květen 2024].
13. CONCEPT ZERO. *A brief history of ferrofluid*. 2014. <http://www.czferro.com/news1/2014/10/27/history-of-ferrofluids/>. Dostupné z: <http://www.czferro.com/news1/2014/10/27/history-of-ferrofluids/> [Citováno: 10. květen 2024].

14. GONCALVES, Fernando D. *Characterizing the Behavior of Magnetorheological Fluids at High Velocities and High Shear Rates*. 2005. <https://api.semanticscholar.org/CorpusID:138145891>. PhD thesis.
15. POLCAR, Petr. *Elektromechanický systém s magnetickou kapalinou*. Plzeň, 2013. [https://dspace5.zcu.cz/bitstream/11025/12693/1/Polcar\\_Petr\\_disertacni\\_prace.pdf](https://dspace5.zcu.cz/bitstream/11025/12693/1/Polcar_Petr_disertacni_prace.pdf). PhD thesis. Západočeská univerzita v Plzni, Fakulta elektrotechnická. Supervised by Prof. Ing. DrSc. MAYER Daniel. Disertační práce.
16. CHIRIKOV, Dmitry; ISKAKOVA, Larisa; ZUBAREV, Andrey; RADIONOV, Alexander. On the theory of rheological properties of bimodal magnetic fluids. *Physica A: Statistical Mechanics and its Applications*. 2014, vol. 406, pp. 298–306. ISSN 0378-4371. Available from DOI: 10.1016/j.physa.2014.03.026.
17. NGUYEN, N. T. Micro-magnetofluidics: interactions between magnetism and fluid flow on the microscale. *Microfluid Nanofluid*. 2012, vol. 12, pp. 1–16. Available from DOI: 10.1007/s10404-011-0903-5.
18. PREMALATHA, Elizabeth S.; CHOKKALINGAM, R.; MAHENDRAN, M. Magneto Mechanical Properties of Iron Based MR Fluids. *American Journal of Polymer Science*. 2012, vol. 2, no. 4, pp. 50–55. Available from DOI: 10.5923/j.ajps.20120204.01.
19. BELL, Richard; ZIMMERMAN, Darin; WERELEY, Norman. Impact of Nanowires on the Properties of Magnetorheological Fluids and Elastomer Composites. In: *Title of the Book*. Ed. by NAME, Editor's. Location: Publisher Name, 2010, Start Page–End Page. ISBN 978-953-7619-88-6. Available from DOI: 10.5772/39480.
20. LU, H. A.; SALABAS, E. L.; SCHÜTH, F. Magnetic Nanoparticles: Synthesis, Protection, Functionalization, and Application. *Angew. Chem. Int. Ed.* 2007, vol. 46, pp. 1222–1244. [https://www.academia.edu/1082928/Magnetic\\_nanoparticles\\_synthesis\\_protection\\_functionalization\\_and\\_application](https://www.academia.edu/1082928/Magnetic_nanoparticles_synthesis_protection_functionalization_and_application). Dostupné z: [https://www.academia.edu/1082928/Magnetic\\_nanoparticles\\_synthesis\\_protection\\_functionalization\\_and\\_application](https://www.academia.edu/1082928/Magnetic_nanoparticles_synthesis_protection_functionalization_and_application) [Citováno: 10. květen 2014].
21. BUTZ, T.; STRYK, O. von. Modelling and Simulation of Electro- and Magnetorheological Fluid Dampers. *ZAMM - Journal of Applied Mathematics and Mechanics / Zeitschrift für Angewandte Mathematik und Mechanik*. 2002, vol. 82, no. 1, pp. 3–20. Available from DOI: 10.1002/1521-4001(200201)82:1<3::AID-ZAMM3>3.0.CO;2-0.
22. JANČÍK, Kryštof. *Návrh hydrodynamické ucpávky axiálního čerpadla s prstencovým motorem*. Brno, 2018. <http://hdl.handle.net/11012/82316>. Diplomová práce. Vysoké učení technické v Brně, Fakulta strojního inženýrství, Energetický ústav. Supervised by František POCHYLÝ. Online zdroj, přístupováno 2024-04-22.
23. KCIUK, Monika; TURCZYN, Roman. Properties and Application of Magnetorheological Fluids. *Journal of Achievements in Materials and Manufacturing Engineering*. 2006, vol. 18.
24. GOŁDASZ, J.; SAPIŃSKI, B. *Erratum to: MR Fluids*. Cham: Springer International Publishing, 2015.
25. GOLDASZ, Janusz; SAPIŃSKI, Bogdan. Magnetostatic Analysis of a Pinch Mode Magnetorheological Valve. *Acta Mechanica et Automatica*. 2017, vol. 11. Available from DOI: 10.1515/ama-2017-0035.

26. GOLDASZ, Janusz; SAPIŃSKI, Bogdan; KUBÍK, Michal; MACHACEK, Ondrej; BANKOSZ, Wojciech. PINCH MODE MAGNETORHEOLOGICAL FLOW BENCH: FLUID FLOW ANALYSIS. 2023, pp. 1373–1380. Available from DOI: 10.7712/150123.9909.445245.
27. ŽÁČEK, Jiří; GOLDASZ, Janusz; SAPIŃSKI, Bogdan; SEDLAČÍK, Michal; STRECKER, Zbyněk; KUBÍK, Michal. Assessment of the Dynamic Range of Magnetorheological Gradient Pinch-Mode Prototype Valves. *Actuators*. 2023, vol. 12, no. 12. ISSN 2076-0825. Available from DOI: 10.3390/act12120449.
28. ELVEFLOW. *Microfluidics: A general overview of microfluidics*. 2019-08. <https://www.elveflow.com/microfluidic-reviews/general-microfluidics/a-general-overview-of-microfluidics/>. [cit. 2024-05-15].
29. MATHUR, Ashish; ROY, Souradeep. Microfluidics and lab-on-a-chip. In: *Electrochemical Sensors*. Elsevier, 2022, pp. 261–287. ISBN 9780128231487. Available from DOI: 10.1016/B978-0-12-823148-7.00010-6. [cit. 2023-03-07].
30. ELVEFLOW. *Microfluidics and microfluidic devices: a review*. 2020-01. <https://www.elveflow.com/microfluidic-reviews/generalmicrofluidics/microfluidics-and-microfluidic-device-a-review/>. [cit. 2024-05-15].
31. RAPP, Bastian E. Introduction. In: *Microfluidics: Modelling, Mechanics and Mathematics*. Elsevier, 2017, pp. 3–7. ISBN 9781455731411. Available from DOI: 10.1016/B978-1-4557-3141-1.50001-0. [cit. 2023-03-07].
32. TABELING, Patrick. *Introduction to Microfluidics*. New York: Oxford University Press, 2005. ISBN 978-0-19-856864-3.
33. NGUYEN, Nam-Trung; WERELEY, Steven T. *Fundamentals and Applications of Microfluidics*. 2nd. Boston: Artech House, 2006. ISBN 978-1-58053-972-2.
34. NGUYEN, Nam-Trung. Micro-magnetofluidics: interactions between magnetism and fluid flow on the microscale. *Microfluidics and Nanofluidics*. 2012, vol. 12, pp. 1–16. Available from DOI: 10.1007/s10404-011-0903-5.
35. BRITANNICA. *Laminar Flow*. n.d. <https://www.simscale.com/docs/simwiki/cfd-computational-fluid-dynamics/what-is-laminar-flow/>. [cit. 2023-03-07].
36. KARNIADAKIS, George; BEŞKÖK, Ali; ALURU, Narayana Rao. *Microflows and Nanoflows: Fundamentals and Simulation*. Vol. xxi. New York: Springer, 2005. Interdisciplinary Applied Mathematics. ISBN 03-872-2197-2.
37. FORMLABS. *Microfluidics vs. Millifluidics: Lab-on-a-Chip Manufacturing*. 2021. <https://formlabs.com/eu/blog/microfluidics-millifluidics-lab-on-a-chip-manufacturing/>. [cit. 2024-05-15].
38. ELVEFLOW. *Introduction to Lab-on-a-Chip: Review, History and Future*. 2020. <https://www.elveflow.com/microfluidic-reviews/general-microfluidics/introduction-to-lab-on-a-chip-review-history-and-future/>. Accessed: 2024-05-15.
39. JORDAN, Andreas; SCHOLZ, Regina; WUST, Peter; FÄHLING, Horst; FELIX, Roland. Magnetic fluid hyperthermia (MFH): Cancer treatment with AC magnetic field induced excitation of biocompatible superparamagnetic nanoparticles. *Journal of Magnetism and Magnetic Materials*. 1999, vol. 201, no. 1, pp. 413–419. ISSN 0304-8853. Available from DOI: 10.1016/S0304-8853(99)00088-8.

40. TOMIOKA, Jun; MIYANAGA, Norifumi. Blood sealing properties of magnetic fluid seals. *Tribology International*. 2017, vol. 113, pp. 338–343. ISSN 0301-679X. Available from DOI: 10.1016/j.triboint.2016.12.040. 43rd Leeds - Lyon Symposium on Tribology 2016.
41. MITAMURA, Yoshinori; YANO, Tetsuya; NAKAMURA, Wataru; OKAMOTO, Eiji. A magnetic fluid seal for rotary blood pumps: Behaviors of magnetic fluids in a magnetic fluid seal. *Bio-medical Materials and Engineering*. 2013, vol. 23, pp. 63–74. Available from DOI: 10.3233/BME-120733.
42. CHEN, J. Z.; LIAO, W. H. Design, testing and control of a magnetorheological actuator for assistive knee braces. *Smart Materials and Structures*. 2010, vol. 19, no. 3, p. 035029. Available from DOI: 10.1088/0964-1726/19/3/035029.
43. *Ferrofluid Audio* [online]. Ferrotec, 2024. [visited on 2024-04-22]. <https://ferrofluid.ferrotec.com/products/ferrofluid-audio/>. Accessed: 2024-04-22.
44. RAJ, K.; MOSKOWITZ, B.; CASCIARI, R. Advances in ferrofluid technology. *Journal of Magnetism and Magnetic Materials*. 1995, vol. 149, no. 1, pp. 174–180. ISSN 0304-8853. Available from DOI: 10.1016/0304-8853(95)00365-7. Proceedings of the Seventh International Conference on Magnetic Fluids.
45. LI, Decai; LI, Yanwen; LI, Zixian; WANG, Yuming. Theory Analyses and Applications of Magnetic Fluids in Sealing. *Friction*. 2023, vol. 11, no. 10, pp. 1771–1793. Available from DOI: 10.1007/s40544-022-0676-8.
46. LIU, B.; LI, W. H.; KOSASIH, P. B.; ZHANG, X. Z. Development of an MR-brake-based haptic device. *Smart Materials and Structures*. 2006, vol. 15, no. 6, p. 1960. Available from DOI: 10.1088/0964-1726/15/6/052.
47. HU, Guoliang; WU, Lifan; LI, Linsen. Torque Characteristics Analysis of a Magnetorheological Brake with Double Brake Disc. *Actuators*. 2021, vol. 10, p. 23. Available from DOI: 10.3390/act10020023.
48. MCDONALD, Kevin; RENDOS, Abigail; WOODMAN, Stephanie; BROWN, Keith; RANZANI, Tommaso. Magnetorheological Fluid-Based Flow Control for Soft Robots. *Advanced Intelligent Systems*. 2020, vol. 2. Available from DOI: 10.1002/aisy.202000139.
49. OH, Jong-Seok; CHOI, Seung-Bok. Ride Quality Control of a Full Vehicle Suspension System Featuring Magnetorheological Dampers With Multiple Orifice Holes. *Frontiers in Materials*. 2019, vol. 6. ISSN 2296-8016. Available from DOI: 10.3389/fmats.2019.00008.
50. STIFTER, Jakub. *Experimentální studium nestabilit mazacího filmu kluzného ložiska*. Brno, 2018. Diplomová práce. Vysoké učení technické v Brně, Fakulta strojního inženýrství. Vedoucí diplomové práce Ing. Milan Omasta, Ph.D.
51. MUSZYŃSKA, Agnieszka. Whirl and whip – Rotor/bearing stability problems. *Journal of Sound and Vibration*. 1986, vol. 110, no. 3, pp. 443–462. ISSN 0022-460X.
52. NEWKIRK, B. L.; TAYLOR, H. D. Shaft whipping due to ill action in journal bearings. *General Electric Review*. 1925, vol. 28, no. 8, pp. 559–568.
53. HORI, Y. A Theory of oil whip. *ASME Journal of Applied Mechanics*. 1959, vol. 26, no. 2, pp. 189–198.

54. SADABADI, Hamid; SANATI NEZHAD, Amir. Nanofluids for Performance Improvement of Heavy Machinery Journal Bearings: A Simulation Study. *Nanomaterials*. 2020, vol. 10, no. 11. ISSN 2079-4991. Available from DOI: 10.3390/nano10112120.
55. TAO, L. N. GENERAL SOLUTION OF REYNOLDS EQUATION FOR A JOURNAL BEARING OF FINITE WIDTH. *Quarterly of Applied Mathematics* [online]. 1959, vol. 17, no. 2, pp. 129–136 [visited on 2024-05-13]. ISSN 0033569X, ISSN 15524485. <http://www.jstor.org/stable/43634920>.
56. BERRY, J. E. *Oil whirl and Whip Instabilities – Within Journal Bearings* [Dostupné na: [www.machinerylubrication.com](http://www.machinerylubrication.com)]. Neuvedeno. Dostupné online [datum přístupu: 24. 01. 2024].
57. KUČERA, Ondřej. *Realizace edukačních úloh na experimentálních stanicích pro kluzná ložiska mazaná olejem a vzduchem*. Brno, 2010. Diplomová práce. Vysoké učení technické v Brně, Fakulta strojního inženýrství. Vedoucí diplomové práce Ing. Michal Vaverka, Ph.D.
58. BILOŠ, Jan; BILOŠOVÁ, Alena. *Aplikovaný mechanik jako součást týmu konstruktérů a vývojářů: Vibrační diagnostika*. Ostrava, 2012. <http://projekty.fs.vsb.cz/147/ucebniopory/978-80-248-2755-1.pdf>. [cit. 2024-05-15].
59. STACHOWIAK, G. W.; BATCHELOR, A. W. *Engineering Tribology*. Fourth. Oxford: Elsevier/Butterworth-Heinemann, 2014. ISBN 978-0-12-397047-3.
60. MEEKER, David. *FEMM User's Manual*. FEMM, 2020. <https://www.femm.info/wiki/Documentation/>. Online; accessed 10-May-2024.
61. WIDODO, P. J.; BUDIANA, E. P.; UBAIDILLAH; IMADUDDIN, F. Magnetically-Induced Pressure Generation in Magnetorheological Fluids under the Influence of Magnetic Fields. *Applied Sciences*. 2021, vol. 11, p. 9807. Available from DOI: 10.3390/app11219807.
62. GERSHTEIN, Sergey; GERSHTEIN, Anna. *Convert American Wire Gauge, AWG to British Standard Wire Gauge, SWG*. 2024. [https://www.convert-me.com/en/convert/wire\\_gauge/gaugeAWG/gaugeAWG-to-gaugeSWG.html](https://www.convert-me.com/en/convert/wire_gauge/gaugeAWG/gaugeAWG-to-gaugeSWG.html). Accessed: 2024-05-23.
63. BARCÍK, Štefan; NEUPAUEROVÁ, Andrea; KOLEDA, Pavol; SUJOVÁ, Erika; MINÁRIK, Marián. *Katalóg zariadení*. Zvolen: Vydavateľstvo Technickej univerzity vo Zvolene, 2016. ISBN 978-80-228-2869-7.
64. ČECH, J.; PERNIKÁŘ, J.; PODANÝ, K. *Strojírenská metrologie*. 4. přepracované vydání. Brno: Akademické nakladatelství CERM s.r.o., 2005. ISBN 80-214-3070-2.
65. *Fluid Control Valves* [online]. Aignep, 2024. [visited on 2024-04-22]. <https://b2b.aignep.com/eng/Fluid-control-valves>. Accessed: 2024-04-22.
66. CORPORATION, LORD. *MRF-132DG Magneto-Rheological Fluid - 1 Liter* [online]. ShopLORDMR, 2024. [visited on 2024-04-22]. <https://www.shoplordmr.com/mr-products/mrf-132dg-magneto-rheological-fluid-1-liter>. Accessed: 2024-04-22.
67. WIDODO, Prabowo Joko; BUDIANA, Edi Purwanto; UBAIDILLAH, Ubaidillah; IMADUDDIN, Faiz; CHOI, Seung-Bok. Effect of Time and Frequency of Magnetic Field Application on MRF Pressure Performance. *Micromachines*. 2022, vol. 13, no. 2, p. 222. Available from DOI: 10.3390/mi13020222.

68. WIDODO, Purwadi Joko; BUDIANA, Eko Prasetya; UBAIDILLAH; IMADUDDIN, Fitriani. New operating mode of magnetorheological fluids (MRFs) simulation studies with finite element methods for magnetics (FEMM). In: *AIP Conference Proceedings*. 2023, vol. 2674, p. 030039. No. 1. Available from DOI: 10.1063/5.0119051.
69. OSTADFAR, Ali. Fluid Mechanics and Biofluids Principles. In: *Biofluid Mechanics: Principles and Applications*. Elsevier, 2016, pp. 1–60. ISBN 9780128024089. Available from DOI: 10.1016/B978-0-12-802408-9.00001-6.

# List of Figures

1.1.1 A comparison of magnetic field lines of magnetic flux density $\vec{B}$ , magnetic field strength $\vec{H}$ and magnetisation $\vec{M}$ inside and outside a cylindrical bar magnet [7](edited) . . . . .	20
1.1.2 A visualisation of magnetic pole models (from left to right): a magnetic dipole; an attraction of opposite poles; a repulsion of the same poles [8](edited) . . . . .	22
1.2.1 Different types of magnetic behaviour [5] . . . . .	25
1.2.2 Domain structure of magnetic substance [4] . . . . .	26
1.3.1 The hysteresis curve [3] . . . . .	26
1.3.2 Hysteresis curve for hard and soft magnetic materials [5] . . . . .	27
2.1.1 Schematic of magnetic particles with surfactant (purposefully not in scale for clarity) [9] . . . . .	30
2.2.1 A Schematic of the described effects [19] . . . . .	30
2.4.1 Fluid flow of magnetorheological liquid through fixed parallel plates [14] . . . . .	32
2.4.2 Schematic of valve mode [5] . . . . .	33
2.4.3 Schematic of shear mode [5] . . . . .	34
2.4.4 Schematic of squeeze mode [5] . . . . .	34
2.4.5 Schematic of shear mode [27] . . . . .	35
3.3.1 Micromagnetofluidics, its subfields and representative applications [34] . . . . .	38
4.1.1 (a) magnetocaloric pump; (b) annular pump with two ferromagnetic liquid pumps; (c) annular pump with one ferromagnet liquid pump; (d) peristaltic pump; (e) pump with three ferromagnetic liquid valves; (f) pump with check valves and ferromagnetic liquid piston; (g) stepper pump with ferromagnetic liquid [34] . . . . .	40
4.2.1 Schematic of an audio speaker with ferromagnetic liquid [43] . . . . .	41
4.2.2 Schematic of the magnetic liquid sealing [45] . . . . .	41
4.2.3 (a) three-dimensional model and (b) material distribution of the MR brake [47] . . . . .	42
4.2.4 Schematic showing magnetic field placement to independently control the motion of two actuators; the MR fluid is continuously flowing from the top (orange arrow) [48] (edited) . . . . .	42
4.2.5 Schematic of a MR damper [49] . . . . .	43
4.3.1 Schematic of journal bearing [54] . . . . .	44
4.3.2 Development of the oil whirl followed by the oil whip [58] . . . . .	45
4.3.3 Typical geometries employed for instabilities precaution; (a) three-lobed; (b) half-lemon; (c) lemon; (d) displaced (in some literature also as offset); (e) spiral [59] . . . . .	46



5.0.1 Schematic of the simulations process . . . . .	47
5.1.1 The B-H curve of MRF-132DG plotted by the FEMM software . . . . .	50
5.1.2 The contours of flux magnitude the case $d_{in} = 2,4$ mm, $I = 0,25$ A . . . . .	51
5.1.3 Comparison of results between the inner diameters in the axsymmetric simulation	51
5.1.4 Comparison of results between the inner diameters in the planar simulation . .	52
5.1.5 Comparison of results between the axisymmetric and planar cases . . . . .	52
5.2.1 Schematic of geometry and named selections (purposefully not in scale for the sake of clarity) . . . . .	53
6.1.1 The UMK-type micromanometer with an inclined tube used in our experiment.	56
6.1.2 Schematic of the inclined tube micromanometer [64] . . . . .	57
6.2.1 The solenoid valve coil SOL10012C4000 X1F series from AIGNEP manufacturer [65] . . . . .	58
6.2.2 Coil measurement scheme . . . . .	60
6.2.3 Coil measurement with Hall probe . . . . .	60
6.2.4 FEMM simulation result for the case $I = 1$ A . . . . .	61
6.2.5 Comparison results between the teslameter measurement and simulation . . . .	61
6.2.6 Measurement of the second coil with properties $N=100$ , $d_w=2$ mm (AWG 12), $d_{in}=2$ cm at $I=0,06$ A, $B=3,14$ mT . . . . .	62
6.3.1 B-H curve of the magnetorheological liquid MRF-132DG [66] . . . . .	63
6.3.2 The relationship between yield stress $\tau_y$ and magnetic field strength $\vec{H}$ of the magnetorheological liquid MRF-132DG [66] . . . . .	64
6.4.1 The configuration by authors [61], [67] and [68] . . . . .	65
6.4.2 The configuration by us . . . . .	65
6.4.3 The test with Teslameter and test simulation in FEMM software by [61], [67] and [68] . . . . .	66
6.4.4 The validation of the measured values and coil simulation [61], [67] and [68] . .	66
6.4.5 The validation of the measured values and coil simulation by us . . . . .	67
6.4.6 Results of the FEMM simulation for the case $I = 1$ A by [61], [67], and [68] . .	67
6.4.7 Our results of the FEMM simulation for $d_{in} = 2,4$ mm, $I = 0,25$ A . . . . .	68
6.4.8 The correlation between magnetic induction and current from FEMM simulation by [61], [67] and [68] . . . . .	68
6.4.9 The correlation between magnetic induction and current from FEMM simulation by us . . . . .	69
7.2.1 Suggested concepts of journal bearing with magnetorheological liquid in micro- or millichannels, from left to right: (a) Channels in the axial direction with a circumferential angle of $120^\circ$ ; (b) Channels in the radial direction; (c) Multiple channels in the radial direction. . . . .	71

# List of Tables

1.3.1 Brief overview of magnetic properties between hard and soft magnetic materials [5] . . . . .	27
3.4.1 An overview of the arguments . . . . .	38
5.2.1 An overview of different configurations of setups . . . . .	55
6.2.1 Parameters known from the provider . . . . .	58
6.2.2 Parameters measured manually . . . . .	58
6.2.3 Constants relevant for the coil calculation . . . . .	59
6.2.4 Calculated quantities . . . . .	59
6.4.1 where $\Delta P_{min}$ is the minimum pressure change that occurs during magnetisation at the observation cycle at each given current, $\Delta P_{max}$ is the maximum pressure change that occurs during magnetisation at the observation cycle at each given current, $\Delta P_{avg}$ is the average pressure change that occurs during magnetisation at the observation cycle, Std Deviation is the standard deviation of the measured pressure. . . . .	69

# Nomenclature

$d$	diameter, characteristic dimension	[m]
$d_{in}$	inner diameter	[m]
$d_{out}$	outer diameter	[m]
$d_{eff}$	effective diameter	[m]
$d_w$	wire diameter	[m]
$e$	conversion rate	[-]
$f$	frequency	[Hz]
$g$	gravitational acceleration	[m.s <sup>-2</sup> ]
$h$	film thickness	[m]
$\vec{j}$	current density	[A.m <sup>-2</sup> ]
$l$	length	[m]
$\ell$	curve	[m]
$p_1, p_2$	pressure	[Pa]
$\Delta p$	pressure difference	[Pa]
$t$	width of the winding	[m]
$q$	particle charge	[C]
$t$	width of the winding	[m]
$\vec{v}$	velocity	[m.s <sup>-1</sup> ]
$\vec{A}$	magnetic vector potential	[-]
$\vec{B}$	magnetic flux density or magnetic induction	[T]
$\vec{D}$	electric flux density	[Vm]
$\vec{E}$	electric field intensity	[m.s <sup>-1</sup> ]
$\vec{F}_L$	Lorentz force	[N]

$\vec{H}$	magnetic field strength or intensity of magnetic field	[A/m]
$\vec{H}_C$	magnetic coercivity	[A/m]
$I$	current	[A]
$L$	deflection of the liquid in the tube	[m]
$\mathcal{L}$	inductance	[H]
$\vec{M}$	magnetisation or dipole moment density	[A.m <sup>-1</sup> ]
$\vec{M}_0$	spontaneous magnetisation	[A.m <sup>-1</sup> ]
$\vec{M}_S$	saturation magnetisation	[A.m <sup>-1</sup> ]
$\vec{M}_R$	remanent magnetisation	[A.m <sup>-1</sup> ]
$N$	number of turns	[-]
$\vec{P}$	magnetic polarisation vector	[T]
$S$	surface	[m <sup>2</sup> ]
$S_1$	cross-section of the vessel	[m <sup>2</sup> ]
$S_2$	cross-section of the tube	[m <sup>2</sup> ]
$P$	power	[W]
$R$	resistance	[Ω]
$U$	voltage	[V]
$\tilde{U}$	relative velocity of bearing surfaces	[m.s <sup>-1</sup> ]
$\dot{\gamma}$	shear strain	[s <sup>-1</sup> ]
$\eta$	dynamic viscosity	[Pa.s]
$\mu$	permeability	[H.m <sup>-1</sup> ]
$\mu_0$	vacuum permeability	[H.m <sup>-1</sup> ]
$\mu_r$	relative permeability	[-]
$\rho_e$	charge density	[C.m <sup>-1</sup> ]
$\rho$	fluid density	[kg.m <sup>-3</sup> ]
$\tilde{\rho}$	electrical resistivity	[Ω.m]
$\tau_y$	yield stress	[Pa]
$\tau$	shear stress	[Pa]
$\varphi$	angle	[°]

$\vec{\Phi}$	magnetic flux	[Wb]
$\chi_m$	magnetic susceptibility	[-]
$Re$	Reynolds number	[-]

# Appendices

## MATLAB Code for the Coil

```
% INPUT
B = 3e-3; % Magnetic Flux Density (T)
I = 1; % Current (A)
l = 22; % Length of the Coil (mm)
d_in = 10.2e-3; % Inner Diameter of the Coil (mm)
L = 8.821e-3; % Inductance (H)
R = 21.6; % Resistance (Ohm)
rho = 1.69e-8; % Resistivity of Copper (Ohm*m)
mu_0 = 4 * pi * 10^-7; % Vacuum's Permeability (H/m)

% Calculate the number of turns
N = (B*l*1e-3)/(mu_0*I);

% Calculate the diameter of the wire [mm]
d_wire = (l/N);

% Calculate the diameter of the wire
t=((2*d_wire*N)/l);

% Calculate the outer diameter of the coil
d_out = (d_in+2*t);

% RESULTS
fprintf('Winding: %.2f\n', N);
fprintf('Wire Diameter: %.6f mm\n', d_wire);
fprintf('Width: %.6f mm\n', t);
fprintf('Outer Diameter: %.6f mm\n', d_out);
```

## ANSYS Fluent UDF Codes

### UDF for the Bingham model

```
#include "udf.h"
#define muOFF (0.092)
#define tauY (33000)

DEFINE_PROPERTY(apparent_vis_2A_1000_0092, c, t)
{
    real x[ND_ND];
    real mu_ef;
    real gamma = C_STRAIN_RATE_MAG(c, t);

    if (gamma != 0.0)
    {
        mu_ef = muOFF + tauY / gamma;
    }
    else
    {
        mu_ef = 1000;
    }

    return mu_ef;
}
```

### UDF for the Mesh Movement

```
#include "udf.h"

real v;
real f;

DEFINE_CG_MOTION(ten,dt,vel,omega,time,dttime)
{
    NV_S(vel, =, 0.0);
    NV_S(omega, =, 0.0);

    f = 0.0025;
    v = 0.03*2*M_PI*f*cos(2*M_PI*f*time);
    vel[1] = v;
}
```